

Pentagram Rigidity for Centrally Symmetric Octagons

Richard Evan Schwartz *

January 17, 2024

Abstract

In this paper I will establish a special case of a conjecture that intertwines the deep diagonal pentagram maps and Poncelet polygons. The special case is that of the 3-diagonal map acting on affine equivalence classes of centrally symmetric octagons. The proof involves establishing that the map is Arnold-Liouville integrable in this case, and then exploring the Lagrangian surface foliation in detail.

1 Introduction

Given an n -gon P_0 , we let $P_1 = T_k(P_0)$ be the n -gon obtained by intersecting the successive k -diagonals of P_0 . For $k = 2$ the map T_k is known as the *pentagram map* and it is a well-studied dynamical system. When $k > 2$ the map is often called a *deep diagonal map*. Figure 1 below shows two examples of the 3-diagonal map T_3 acting on 8-gons. The map T_k is generically defined and invertible. The deep diagonal maps are amongst the simplest of many generalizations of the pentagram map. See e.g. [3], [4], [5], [7], [8], [9], [11], [12], [13], [14], [15], [18], [19], [20], [25], [26] for results about the pentagram map and its generalizations.

The diagonal maps interact nicely with Poncelet polygons. A *Poncelet polygon* in the projective plane is a polygon which is inscribed in one conic section and circumscribed about another. Poncelet polygons are classic objects in projective geometry. In [20] I proved that if P is a Poncelet n -gon

*Supported by N.S.F. Grant DMS-2102802

Address: Department of Mathematics, Brown University, 151 Thayer Street, Providence, RI, 02912, USA

Email: Richard.Evan.Schwartz@gmail.com

and n is odd then $T_k(P)$ and P are projectively equivalent. I gave the proof in the odd case just for convenience; I am sure that the result holds in the even case as well.

A polygon in the projective plane is *convex* if it is projectively equivalent to a planar convex polygon. In [7], a much more recent and advanced work, A. Izosimov proves that if P is a convex polygon and $T_2(P)$ is projectively equivalent to P , then P is a Poncelet polygon. This result can fail e.g. for certain non-convex polygons in the complex projective plane.

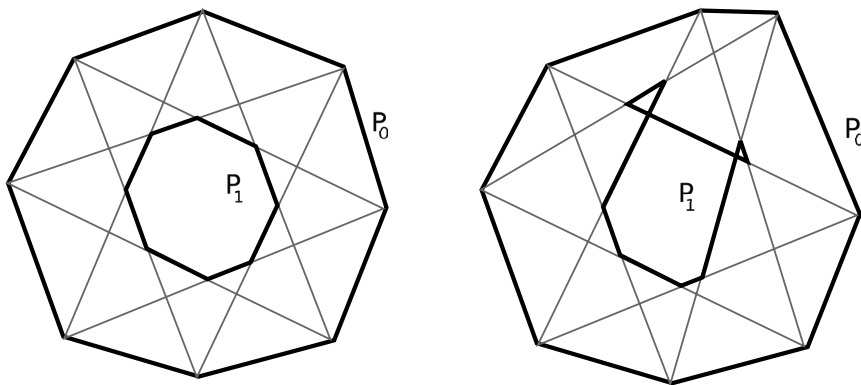


Figure 1: P_0 and $P_1 = T_3(P_0)$.

The maps T_k and T_k^{-1} are always defined on convex n -gons. As Figure 1 shows, the map T_3 need not preserve convexity. Starting with P_0 we define the k -diagonal orbit to be the bi-infinite sequence $\{P_j\}$ where $P_j = T_k^j(P_0)$. My result about Poncelet polygons implies that if P_0 is convex and Poncelet then P_j is convex (and Poncelet) for all $j \in \mathbf{Z}$. Here is a deeper conjecture about how the deep diagonal maps interact with Poncelet polygons – no pun intended.

Conjecture 1.1 (Pentagram Rigidity) *Let (n, k) be relatively prime with $n \geq 7$ and $3 \leq k < n/2$. Let P_0 be a convex n -gon and let $\{P_j\}$ be its k -diagonal orbit. Then P_0 is a convex Poncelet polygon if and only if $\{P_j\}$ is convex for all $j \in \mathbf{Z}$.*

I have been talking, occasionally and informally, about this conjecture for about 35 years but I only recently wrote it down. See Conjecture 7.13 in [21]. Originally I conceived of the Pentagram Rigidity Conjecture as a projective geometry analogue of circle-packing rigidity. The first such circle packing rigidity paper is [16]. See [17] for a much broader and more definitive work on circle packing rigidity.

Let me comment on the constraints on k and n . When $k = 2$ the conjecture fails because T_2 preserves convexity. I did enough experimenting to convince myself (without a formal proof) that when k and n are even, the map T_k^2 is the identity mod scale on semi-regular n -gons. These are polygons with n -fold but not necessarily $2n$ -fold dihedral symmetry. In any case, one can pick a concrete example to furnish a counter-example to the conjecture when k and n are both even. Perhaps the conjecture holds in the more general situation that k and n are not both even, but I would prefer to make a more cautious conjecture.

In [22] I proved Conjecture 1.1 for the case of 8-gons with 4-fold rotational symmetry. In this toy case, the relevant moduli space is 2-dimensional and foliated by T_3 -invariant elliptic curves. The other “simplest case”, that of 7-gons with bilateral symmetry, is similar.

In this paper I will prove the first really nontrivial case of the conjecture. An even-sided polygon P is *centrally symmetric* if it is invariant with respect to the map $p \rightarrow -p$.

Theorem 1.2 (Main) *The Pentagram Rigidity Conjecture is true for $(8, 3)$ provided that the octagon is centrally symmetric.*

This case is attractive for two reasons. First, the analysis goes beyond elliptic curves. Second, this is the first case in which the full Poncelet families arise. Very few Poncelet 8-gons have 4-fold symmetry, but all Poncelet 8-gons (and indeed all even-sided Poncelet polygons) are centrally symmetric. See [6].

Our proof will show the stronger result that the forward orbit remains convex if and only if P_0 is inscribed in an ellipse. It is already a theorem in [2] that if an octagon (not necessarily centrally symmetric) is inscribed in an ellipse then so is its image under T_3 . See also [23]. In §7, when I treat the case of inscribed and circumscribed 8-gons, I will obtain the following additional result about the inscribed case.

Theorem 1.3 *Let P_0 be a convex centrally symmetric 8-gon which is not Poncelet but which is still circumscribed about an ellipse. Then P_k converges to a convex Poncelet 8-gon as $k \rightarrow \infty$ and (if the iterates are all defined) to a star-convex Poncelet 8-gon as $k \rightarrow -\infty$. Up to affine transformation, the two limits have the same vertex set and the vertex orders are related by the star-reordering: $12345678 \rightarrow 14725836$.*

The Main Theorem derives from a structural result about T_3 . Let $\mathcal{P}_{8,2}$ denote the space of affine equivalence classes of centrally symmetric 8-gons. We choose coordinates so that $\mathcal{P}_{8,2}$ is an open dense subset of \mathbf{R}^4 .

Theorem 1.4 (Integrability) *The action of T_3 on the 4-dimensional space $\mathcal{P}_{8,2}$ has an invariant (singular) symplectic form and 2 algebraically independent rational invariants which Poisson commute with respect to it.*

I found the invariant symplectic form and the algebraic invariants by guesswork, and then their verification is quite straightforward. At the end of §2.3 I will give more motivation and relate the invariants somewhat to the literature. Integrability is a main theme in the study of T_2 , and indeed the pentagram map is one of the best known discrete completely integrable systems. Certain integrability results are known for T_k for all $k \geq 2$. It is proved in [5] that T_k is completely integrable when defined on the space of so-called *twisted, corrugated* polygons. A general integrability result, Theorem 6.2 in [9], covers the action of T_3 on the space of projective classes of ordinary polygons, but it seems difficult to extract from [5] and [9] an explicit integrability result like Theorem 1.4. Interestingly, one also sees integrable systems arise in circle packings. There are a number of works about this; see e.g. [1].

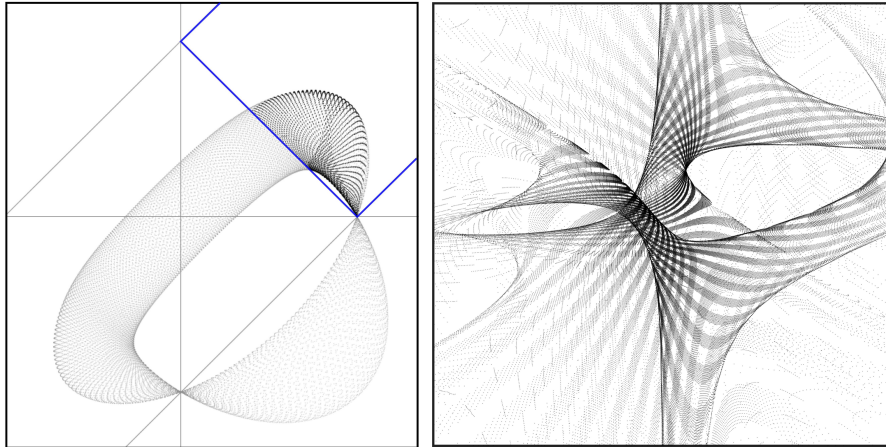


Figure 2: A torus orbit and a beautiful orbit.

Figure 2 (left) illustrates how Theorem 1.4 helps prove the Main Theorem. This picture shows a planar projection of the first 2^{15} points of an orbit that starts with a point representing a convex 8-gon. The metric completion of the orbit is a torus. The darkly shaded part of the orbit is (as we prove) a cylinder L_+ which properly contains a subset $C_+ \subset L_+$ of points representing convex 8-gons. Even if a point starts out representing a convex

polygon, the torus motion eventually moves the point outside the region where it is convex – unless it is Poncelet to begin with.

An earlier version of this paper showed that the metric completions of orbits like the one shown on the left in Figure 2 are flat tori. However, when revising the paper, I found a shorter proof which only requires an analysis of the pair (C_+, L_+) . For the interested reader, I discuss the torus construction without proof in §6.4

Figure 2 (right) shows a planar projection of the first 2^{19} points of an orbit that does not contain points representing convex 8-gons. This orbit appears to lie on a higher genus surface with a singular flat structure. This kind of orbit is not relevant for our analysis but it makes a beautiful picture and hints at some additional structure to be explored.

This paper is organized as follows. In §2 I will prove Theorem 1.4 and introduce most of the main players in the game. In §2.8 I give a 6-step outline of the proof of the Main Theorem. The rest of the paper carries out the steps of the outline.

Why is this paper so long? The Integrability Theorem has a short and easy proof, but then the troubles begin. Since we need to deal with *every single level set*, the usual appeal to Sard’s Theorem in this situation is not of any help. We need to use some computer algebra to check by hand that every single level set containing convex points is smooth. Also, the level sets degenerate at either end in \mathbf{R}^4 so we have to understand the way this happens and deal with it. Finally, we need fairly fine information about the level sets: They are topological cylinders whose metric boundaries, with respect to the intrinsic flat structure coming from integrability, is locally concave away from 2 points. All of this adds length to the paper.

The interested reader can download the computer program I wrote, which does experiments with the 3-diagonal map on $\mathcal{P}_{8,2}$. See

<http://www.math.brown.edu/~res/Java/OCTAGON.tar>

The download also contains a number of Mathematica files I used for most of the calculations in the paper. These files should help the interested reader reproduce the calculations.

1.1 Acknowledgements

I thank Misha Bialy, Dan Cristofaro-Gardiner, Misha Gekhtman, Anton Izosimov, Boris Khesin, Curtis McMullen, Valentin Ovsienko, Dan Reznik, Joe Silverman, Sergei Tabachnikov, and Max Weinreich for helpful conversations. I also thank the anonymous referees for helpful comments.

2 The Main Ideas

2.1 Complete Integrability

We begin with a quick introduction to integrable systems.

Let V be an open subset of \mathbf{R}^4 . Let $F_1, F_2 : V \rightarrow \mathbf{R}$ be smooth functions. The pair $(x_1, x_2) \in \mathbf{R}^2$ is a *regular value* if the following is true: For all $p \in V$ such that $F_1(p) = x_1$ and $F_2(p) = x_2$, the gradients ∇F_1 and ∇F_2 are nonzero and linearly independent. In this case, $\Sigma = F_1^{-1}(x_1) \cap F_2^{-1}(x_2)$ is a smooth surface. We call such a Σ a *regular level set*.

Now suppose ω is a symplectic form on V – i.e., a closed and nondegenerate 2-form. There is a unique vector field X_j such that $\omega(X_j, V) = D_V F_j$. Here $D_V F_j$ is the directional derivative of F_j in the direction of V . The vector field X_j is called the *Hamiltonian vector field* associated to F_j . Because $\omega(X_j, X_j) = 0$, the vector field X_j is tangent to the level set of F_j . Also, the flow generated by F_j preserves ω .

The functions F_1 and F_2 *Poisson commute* if $\omega(X_1, X_2) = 0$ everywhere. The vectors X_1, X_2 are linearly independent at some point iff the gradients $\nabla F_1, \nabla F_2$ are linearly independent at this point. When this happens, the restriction of ω to a regular level set Σ is 0. That is, Σ is *Lagrangian*. The vector fields X_1 and X_2 define commuting flows preserving both Σ and ω .

We can use the commuting flows to define coordinate charts from Σ into \mathbf{R}^2 in a canonical way. We start with some point $p \in \Sigma$, which we map to the origin. Each point $q \in \Sigma$ sufficiently near to p defines two numbers $a_1(p, q)$ and $a_2(p, q)$ such that one can reach q by starting at p and flowing for time $a_1(p, q)$ along X_1 and then for time $a_2(p, q)$ along X_2 . The coordinate chart is given by $q \rightarrow (a_1(p, q), a_2(p, q))$. The commuting nature of the flows combines with the linear independence to show that this map really is a local coordinate chart about p . By construction, the overlap functions for our coordinate chart are translations. Thus Σ has the structure of translation surface (without singular points).

Let us combine all this with dynamics. Let $U \subset V \subset \mathbf{R}^4$ be two open sets and suppose we have a smooth map $T : U \rightarrow V$. Suppose that all of ω, F_1, F_2 are T -invariant. Then $T(\Sigma \cap U) \subset \Sigma$, and $T : \Sigma \cap U \rightarrow \Sigma$ is a translation in these coordinates. In this case we would call T *completely integrable* with respect to the pair (U, V) .

In our case, T is a rational map, and ω, F_1, F_2 will be defined in terms of rational functions. All these objects have singularities; they are only defined on open dense subsets of \mathbf{R}^4 . However, we will always restrict our attention to suitable pairs (U, V) of open sets where everything is everywhere defined.

2.2 The Map in Coordinates

Every member $P \in \mathcal{P}_{8,2}$ has a canonical representative with vertices

$$(1, 0), (a, b), (0, 1), (-d, c), (-1, 0), (-a, -b), (0, -1), (d, -c). \quad (1)$$

We label these vertices v_0, \dots, v_7 . We call $p = (a, b, c, d)$ the *coordinates* of P . When $(a, b) = (c, d)$ our point lies in the space $\mathcal{P}_{8,4}$ of affine equivalence classes of 8-gons with 4-fold rotational symmetry.

When we apply the map T_3 we initially get a polygon P' with vertices v'_0, \dots, v'_7 , where

$$v'_k = \overline{v_{k+1}v_{k+4}} \cap \overline{v_{k+2}v_{k+5}},$$

where the indices are taken mod 8. Then we normalize to get back to Equation 1 and find the new coordinates $(a', b', c', d') = T_3(a, b, c, d)$. One could use other labeling conventions, but this one leads to a nice formula for T_3 . Let $e = ac + bd$.

$$T_3 = A\Delta A\Delta, \quad (2)$$

$$A(a, b, c, d) = (-b, -a, -d, -c), \quad (3)$$

$$\Delta = \left(\frac{b(c+d+1)}{c(e+a+c+1)}, \frac{d(e+b+c)}{c(e+a+c+1)}, \frac{d(a+b+1)}{a(e+a+c+1)}, \frac{b(e+a+d)}{a(e+a+c+1)} \right) \quad (4)$$

The map Δ is nice because all its component functions are positive – it preserves “positivity”. The map $A\Delta A$ is nice because it preserves convexity. See §2.6 below.

We note some useful symmetries. Let \sqrt{I} denote the map we get by replacing the polygon in Equation 1 by the index-shifted polygon

$$(a, b), (0, 1), (-d, c), (-1, 0), (-a, -b), (0, -1), (d, -c), (1, 0)$$

and then renormalizing as in Equation 1. Let $I = \sqrt{I} \circ \sqrt{I}$. Let J be the map which reflects the polygon in the line $y = x$ and then dihedrally relabels the coordinates so that the polygon starts out $(1, 0), (b, a), \dots$. In coordinates (with $e = ac + bd$ again), we have

$$\sqrt{I} = \left(\frac{d}{e}, \frac{a}{e}, \frac{b}{e}, \frac{c}{e} \right), \quad I = (c, d, a, b) \quad J = (b, a, d, c). \quad (5)$$

Here, for the sake of typesetting, we have set $J = J(a, b, c, d)$, etc.

If γ is any composition of these symmetries, then $\gamma(p)$ represents an 8-gon that is an isometric and dihedrally relabeled copy of the one represented by p . The maps \sqrt{I} and I commute with T_3 and J commutes with T_3^2 . These symmetries will sometimes cut down on the number of cases we need to consider.

2.3 Some Important Functions

Let $\mathcal{I} \subset \mathcal{P}_{8,2}$ denote the subset consisting of equivalence classes of 8-gons which are inscribed in a conic section. Let $\mathcal{I}^* \subset \mathcal{P}_{8,2}$ denote the subset consisting of equivalence classes of 8-gons circumscribed about a conic section. Define functions

$$g_{ab}^* = a - b, \quad g_{cd}^* = c - d, \quad g_{ab} = \frac{1 - a^2 - b^2}{ab}, \quad g_{cd} = \frac{1 - c^2 - d^2}{cd}. \quad (6)$$

A computation shows that

$$(a, b, c, d) \in \mathcal{I} \iff g_{ab} + g_{cd} = 0, \quad (a, b, c, d) \in \mathcal{I}^* \iff g_{ab}^* + g_{cd}^* = 0. \quad (7)$$

The first of these equations has a simple geometric interpretation. From the way we have normalized our 8-gons, the point (a, b) lies on the ellipse $x^2 + y^2 + g_{ab}xy = 1$. The point $(-d, c)$ lies on the ellipse $x^2 + y^2 - g_{cd}xy = 1$. If these points lie on the same ellipse then the constants are the same, meaning that $g_{ab} + g_{cd} = 0$. I don't know a nice geometric interpretation for the second equation, but it is an easy calculation. Define

$$G(a, b, c, d) = 2(g_{ab} + g_{cd})(g_{ab}^* + g_{cd}^*). \quad (8)$$

Discussion: (The reader can safely ignore this.) Motivated by Equation 7 I guessed that G is a T_3 invariant. Motivated by the literature on the pentagram map, e.g. my paper [19], I then guessed that the polynomial expression $(O_8/E_8)^{1/6}$ is also a T_3 invariant. The functions O_8 and E_8 are (now) called the *odd and even Casimirs* for the T_2 -invariant Poisson structure. Fooling around, I came up with algebraically nicer ones, F_1 and F_2 , described in the next section. The invariants F_1 and F_2 satisfy the relations:

$$F_2 - F_1 = G, \quad \frac{F_1}{F_2} = (O_8/E_8)^{1/6}. \quad (9)$$

According to the anonymous referee, the invariants F_1 and F_2 can be interpreted in terms of previous work [5], [7] on T_3 . In [5], it is shown that there is a (non-invertible) map Φ from planar polygons to corrugated polygons in \mathbf{RP}^3 which intertwines T_3 with the analogous map on corrugated polygons. Pulling back an invariant for corrugated polygons gives an invariant of T_3 on ordinary polygons. Moreover the invariants for T_3 on corrugated polygons can be deduced from the Lax pair in [7]. Here is an example. One can interpret a centrally symmetric octagon as a quadrilateral whose monodromy has eigenvalues $(-1, -1, 1)$. Applying Φ we get a corrugated quadrilateral whose monodromy has eigenvalues $(1, -1, 1, \mu)$. The quantity $1/\mu$ is precisely F_1/F_2 , and the monodromy is an invariant.

2.4 Proof of Theorem 1.4

Let $e = ac + bd$. Our two basic invariants for T_3 are F_1 and F_2 where

$$\begin{aligned} F_1 &= \frac{(1+a-b)(1+c-d)(e+b-c)(e+d-a)}{abcd}, \\ F_2 &= \frac{(1-a+b)(1-c+d)(e-b+c)(e-d+a)}{abcd}. \end{aligned} \quad (10)$$

Referring to the maps in Equation 5, these functions obey the symmetries: $F_j \circ \sqrt{I} = F_j$ and $F_{3-j} = F_j \circ J$. One can calculate in Mathematica directly that F_1 and F_2 are invariants for A and for Δ , and hence for T_3 . One evaluation suffices to check that ∇F_1 and ∇F_2 are linearly independent at some point. Hence F_1 and F_2 are algebraically independent.

The invariant symplectic form is as follows.

$$\omega = \frac{1}{ab} \mathbf{d}a \wedge \mathbf{d}b + \frac{1}{cd} \mathbf{d}c \wedge \mathbf{d}d. \quad (11)$$

One can see directly that $A^*(\omega) = -\omega$. We will describe the calculation that shows $\Delta^*(\omega) = -\omega$. The two facts together imply that ω is T_3 invariant. Let e_1, e_2, e_3, e_4 be the standard basis vectors on \mathbf{R}^4 . Let Ψ denote the Jacobian of Δ , namely the 4×4 matrix of partial derivatives. (To avoid mixing up the matrix with its transpose, let me say that the first column is $\partial\Delta/\partial a$, and the second column is $\partial\Delta/\partial b$, etc.) Let

$$(a', b', c', d') = \Delta(a, b, c, d).$$

We compute

$$\begin{aligned} \Delta^*(\omega)(e_i, e_j) &= \\ \frac{1}{a'b'}(\Psi_{1i}\Psi_{2j} - \Psi_{2i}\Psi_{1j}) + \frac{1}{c'd'}(\Psi_{3i}\Psi_{4j} - \Psi_{4i}\Psi_{3j}) &=^{(!)} \\ -\omega(e_i, e_j). \end{aligned} \quad (12)$$

The equality with an exclamation point is, for each (i, j) , a big Mathematica calculation that miraculously works out.

Given the simple nature of ω we can write down the Hamiltonian vector field X_ϕ for a function $\phi : \mathbf{R}^4 \rightarrow \mathbf{R}$ in an explicit way. We have

$$X_\phi = (-ab\phi_b, ab\phi_a, -cd\phi_d, cd\phi_c). \quad (13)$$

Here $\phi_a = \partial\phi/\partial a$, etc. X_ϕ is defined wherever ϕ is.

Let X_j be the Hamiltonian vector field associated to F_j . Another Mathematica calculation shows that $\omega(X_1, X_2) = 0$. Now we have established all the points of Theorem 1.4.

2.5 Positivity

Let \mathcal{C} be the set of points representing convex 8-gons without 4-fold rotational symmetry. So, we are throwing out points of the form (a, b, a, b) .

Lemma 2.1 (Positivity) *All factors of F_1 and F_2 are positive on \mathcal{C} .*

Proof: Let $(a, b, c, d) \in \mathcal{C}$. The convexity gives the constraints

$$a, b, c, d > 0, \quad |a - b| < 1, \quad |c - d| < 1, \quad a + b > 1, \quad c + d > 1.$$

Let $e = ac + bd$, as in the definition of F_1 and F_2 . To finish the proof we just need to show that the 4 quantities $e + b - c$ and $e - b + c$ and $e + a - d$ and $e + d - a$ are positive. By symmetry it suffices to show $e + b - c > 0$:

$$e + b - c = ac + bd + b - c = (a - 1)c + bd + b > -bc + bd + b = b(d - c + 1) > 0.$$

The first inequality comes from $a + b > 1$ and the second from $d - c > -1$. ♠

Lemma 2.2 *$(a, b, c, d) \in \mathcal{C} - \mathcal{I} - \mathcal{I}^*$ lies on one of four connected components of \mathcal{C} , depending only on the signs of $g_{ab} + g_{cd}$ and $g_{ab}^* + g_{cd}^*$.*

Proof: Let \mathcal{C}' denote the set of all points (a, b, c, d) . The set $\mathcal{C}' - \mathcal{C}$ is a 2-dimensional set where $(a, c) = (b, d)$. This set does not disconnect \mathcal{C}' . Thus, it suffices to prove our result for \mathcal{C}' rather than \mathcal{C} . We claim that the map

$$\psi(a, b, c, d) = (g_{ab}, g_{cd}, g_{ab}^*, g_{cd}^*) = (a', b', c', d')$$

is a homeomorphism – indeed a diffeomorphism – from \mathcal{C}' to the rectangular solid $Q = (-2, 2)^2 \times (-1, 1)^2$. By Equation 7, ψ maps \mathcal{I} and \mathcal{I}^* respectively into the hyperplanes H and H^* given by $a' + b' = 0$ and $c' + d' = 0$. The 4 components of $\mathcal{C}' - \mathcal{I} - \mathcal{I}^*$ are the images of ψ^{-1} of the 4 components of $Q - H - H^*$.

For the homeomorphism claim, it suffice to prove the simpler result that the map

$$(a', c') = \left(\frac{1 - a^2 - b^2}{ab}, a - b \right).$$

is a homeomorphism onto $(-2, 2) \times (-1, 1)$ from set of (a, b) such that $a, b > 0$ and $|a - b| < 1$ and $a + b > 1$. The reason is that a' is the determining coefficient of the ellipse through the points $(\pm 1, 0)$ and $(0, \pm 1)$ containing (a, b) – see the geometric interpretation of g_{ab} given in §2.3 – and c' selects the ray of slope 1, emanating from the line $x + y = 1$, which contains (a, b) . ♠

2.6 Duality and Convexity

In this section we prove the following result

Lemma 2.3 *The map $A\Delta A$ maps \mathcal{C} into itself and preserves the component on which $g_{ab} + g_{cd}$ and $g_{ab}^* + g_{cd}^*$ are positive.*

Proof: Our proof gives an interpretation of $\iota_3 = A\Delta A$ as implementing projective duality. Here is how one represents the line through $p_1 = (x_1, y_1)$ and $p_2 = (x_2, y_2)$.

1. We move to the affine patch in \mathbf{R}^3 by setting $v_j = (x_j, y_j, 1)$.
2. We take the cross product $w = v_1 \times v_2 = (w_1, w_2, w_3)$.
3. We move back to the plane by setting $[p_1, p_2] = (w_1/w_3, w_2/w_3)$.

Concretely, the new point is

$$[p_1, p_2] = \left(\frac{y_1 - y_2}{x_1 y_2 - x_2 y_1}, \frac{x_2 - y_1}{x_1 y_2 - x_2 y_1} \right). \quad (14)$$

Given the polygon P in Equation 1, with successive points P_1, P_2, \dots we define

$$P^* = [P_1, P_2], [P_2, P_3], [P_3, P_4], [P_4, P_5], \dots \quad (15)$$

We then normalize by the needed affine transformation so that the polygon starts out $(1, 0), (a^*, b^*), (0, 1), (-d^*, c^*), \dots$ We write

$$\iota_3^*(a, b, c, d) = (a^*, b^*, c^*, d^*). \quad (16)$$

The dual of a convex octagon is again convex. Hence ι_3^* maps points representing convex octagons to points representing convex octagons. We check that $\iota_3^*(a, b, a, b) = (a^*, b^*, a^*, b^*)$, so that ι_3^* preserves octagons with 4-fold rotational symmetry.

Here is the punchline. We compute that

$$\iota_3 = \iota_3^* \circ I \circ J. \quad (17)$$

Thus ι_3 is the composition of maps which all preserve \mathcal{C} .

Finally, ι_3^* , being a coordinatization of duality, swaps the sets \mathcal{I} and \mathcal{J} . Hence, so does ι_3 . But then ι_3 permutes the 4 components from Lemma 2.2. A single suffices to check that ι_3 preserves the $(+, +)$ component. ♠

Remark: One could prove Lemma 2.3 algebraically, but it is rather tedious.

2.7 Integral Curves

Let $X_G = X_2 - X_1$ be the Hamiltonian vector field associated to $G = F_2 - F_1$. We let \mathcal{X} denote the set of (a, b, c, d) such that

1. a, b, c, d are all nonzero.
2. F_1, F_2, G are all nonzero.
3. $(a, b) \neq (c, d)$. We are throwing out the points corresponding to $\mathcal{P}_{8,4}$.

Lemma 2.4 *In each connected component of \mathcal{X} we can find a smooth function ζ such that $X_G \cdot \nabla \zeta$ does not vanish in that component. In particular, X_G never vanishes on \mathcal{X} .*

Proof: Recall that $G = 2(g_{ab}^* + g_{cd}^*)(g_{ab} + g_{cd}) \neq 0$ on \mathcal{X} . When $ac/bd > 0$ we define $h = \log(ac/bd)$. We compute

$$X_G \cdot \nabla g_{ab}^* = 2(g_{ab}^* + g_{cd}^*)(1 - a + b)(1 + a - b)(a + b)/(ab). \quad (18)$$

$$X_G \cdot \nabla g_{cd}^* = 2(g_{ab}^* + g_{cd}^*)(1 - c + d)(1 + c - d)(c + d)/(cd). \quad (19)$$

$$X_G \cdot \nabla g_{ab} = -2(g_{ab} + g_{cd})(1 - a + b)(1 + a - b)(a + b)/(ab). \quad (20)$$

$$X_G \cdot \nabla g_{cd} = -2(g_{ab} + g_{cd})(1 - c + d)(1 + c - d)(c + d)/(cd). \quad (21)$$

$$X_G \cdot \nabla h = 2(g_{ab}^* + g_{cd}^*)((1 + a^2 + b^2)/(ab) + (1 + c^2 + d^2)/(cd)). \quad (22)$$

Now we observe the following about a component \mathcal{U} of \mathcal{X} .

1. If $ab > 0$ in then $a + b \neq 0$. We can take either $\zeta = g_{ab}$ or $\zeta = g_{ab}^*$.
2. If $cd > 0$ in then $c + d \neq 0$. We can take either $\zeta = g_{cd}$ or $\zeta = g_{cd}^*$.
3. If $ab < 0$ and $cd < 0$ then h is defined in \mathcal{U} and we can take $\zeta = h$.

In all cases we have the desired function. ♠

Say that a G -curve is a maximal curve tangent to X_G . Lemma 2.4 says that \mathcal{X} is foliated by G -curves and that each G -curve γ exits every compact subset of \mathcal{X} at both ends. Why? Because ζ from Lemma 2.4 (which depends on the component of \mathcal{X} that contains γ) is monotone along γ .

Lemma 2.4 has an immediate consequence: At every point of \mathcal{X} , at least one of the vector fields X_1 or X_2 is nonzero. This comes from the fact that $X_G = X_2 - X_1$ is nonzero at each point of \mathcal{X} . In §3 we will give an exact characterization of the locus of points in \mathcal{X} where X_1 and X_2 are linearly independent.

2.8 Proof of the Main Theorem: Outline

Step 1, Linear Independence: Let $\mathcal{X}_+ \subset \mathcal{X}$ denote the subset where all factors of F_1, F_2, G (both in the numerator and in the denominator) are positive. For instance $1 - a + b > 0$ and $a - b + c - d > 0$ on \mathcal{X}_+ . In §3 we prove (as a corollary of an exact characterization) that X_1 and X_2 are linearly independent at every point of \mathcal{X}_+ .

Step 2, The Cylinder and the Nice Loop: Let L_+ be a level set in \mathcal{X}_+ . Let \mathcal{U} denote the set of (a, b, c, d) such that $\max(a + b, c + d) = 1$. In §4, we prove that every G -curve in L_+ intersects \mathcal{U} exactly once, and that $L_+ \cap \mathcal{U}$ is a single loop which we call the *nice loop*. The nice loop is smooth away from the 2 points on it satisfying $a + b = c + d = 1$. We call these points the *corners* of the nice loop. From all this we deduce that L_+ is a cylinder. For points in $\mathcal{P}_{8,4}$, treated in [21], the set L_+ is an arc: a single G -curve.

Step 3, Intrinsic Boundedness and Concavity: In §5 we prove that each level set L_+ in \mathcal{X}_+ is bounded with respect to its intrinsic flat structure coming from its integrability. We also prove that L_+ is locally concave near its intrinsic boundary. We first prove this for the nice loop using calculus, then we show that $\iota_5 = A\Delta A\Delta A$ is an isometry of the sub-cylinder $L'_+ \subset L_+$ bounded by the nice loop and the end of L_+ which abuts $(0, 0, 0, 0)$. The map ι_5 swaps the ends of L'_+ and thus allows us to convert info about the nice loop into info about one end of L_+ . We prove Δ preserves L_+ and swaps its ends. This gives us info about the other end of L_+ .

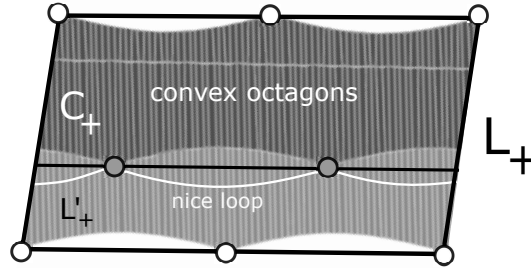


Figure 3: The geometry of L_+ and C_+ when $F_1 = 7/2$ and $F_2 = 4$.

Figure 3 shows a plot of the cylinder L_+ when the invariants are $F_1 = 7/2$ and $F_2 = 4$. The thinner cylinder C_+ is $L_+ \cap \mathcal{C}$. My program integrates the Hamiltonian vector fields and thereby draws a chunk of the universal cover of L_+ . I am showing a fundamental domain. The sides are meant to be identified by translation.

Step 4: The Invariant and the Yardstick: Consider the lift to \mathbf{R}^2 . The horizontal lines in Figure 3 contain the lifts of the corners to \mathbf{R}^2 . We will deduce this from the action of I on the various corners.

We say that the *top line* is the straight line through the lifts of the corners of the end of L_+ that lies on the same side of the nice loop as C_+ . The *bottom line* is defined similarly for the other end of L_+ . We say that the *middle line* is the line through the lifts of the corners on the nice loop. The concavity of the boundary and the properties of the nice loop will imply that the middle line is strictly between the top and bottom lines. Each component of C_+ stretches all the way across and touches both the top line and the middle line. We prove in §6.1 that C_+ is either a cylinder or a pair of disjoint topological disks. Figures 5 and 6 in §6 show cartoon pictures of the disk case.

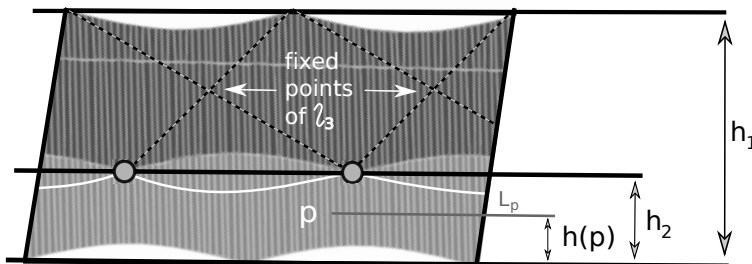


Figure 4: The quantities h_1 and h_2 and $h(p)$.

We let h_1 be the distance between the top and bottom lines. Let h_2 denote the distance between the middle and bottom lines. We have the bounds $0 < h_2 < h_1$. Given $p \in L_+$ we define L_p to be the line through p parallel to the top, bottom, and middle lines, and then we define $h(p)$ to be the distance between the bottom line and L_p . We then define

$$\lambda(p) = \frac{h_2}{h_1} \in (0, 1), \quad \mu(p) = \frac{h(p)}{h_1} \in (0, 1). \quad (23)$$

Any two flat metrics on L_+ are affinely equivalent, so $\lambda(p)$ and $\mu(p)$ only depend on p . The *invariant* $\lambda(\cdot)$ only depends on the level set; it is a function of F_1 and F_2 . The *yardstick function* $\mu(\cdot)$ varies within a level set.

Step 5: The Magic Formula: Because $\iota_3 = A\Delta A$ preserves convexity, and thanks to the topological properties of C_+ established in §6.1, we will show that ι_3 has a lift acting on \mathbf{R}^2 as an order 2 rotation swapping

the top and middle lines. Likewise Δ has the same properties with respect to the top and bottom lines. All this implies *the magic formula*:

$$\mu(T_3^{\pm 1}(p)) = \mu(p) \pm \lambda(C_+). \quad (24)$$

The $(-)$ case holds as long as $p \in C_+$, because then

$$A\Delta A(p) \in C_+, \quad T_3^{-1}(p) = \Delta \circ A\Delta A(p) \in L_+.$$

Both involutions are defined for all relevant points and so the lifts make sense. We can then deduce the $(+)$ case from the $(-)$ case when both p and $T_3(p)$ lie in C_+ . In particular, if the whole orbit lies in C_+ , then both cases of Equation 24 would always hold.

Call an octagon *convex generic* if it is convex, and neither inscribed nor circumscribed, and without 4-fold rotational symmetry. The magic formula has the following immediate application: At most $(1 - \mu)/\lambda$ of the forward T_3 -iterates of p , and at most μ/λ of the backward T_3 -iterates of p , remain in \mathcal{C} . Here we have set $\lambda = \lambda(p)$ and $\mu = \mu(p)$. This application establishes Theorem 1.1 for convex generic octagons represented by points in \mathcal{X}_+ .

If Theorem 1.1 has a counter-example p which is generic convex then, as we show, we can apply some element γ in the group generated by the maps \sqrt{I} and J so that $\gamma(p)$ is represented by a point in \mathcal{X}_+ . Then $\gamma(p)$ would also be a counter-example, a contradiction. This proves Theorem 1.1 in the generic convex case. The case of 4-fold symmetry follows from [21], or else one could view it as an easy limiting case of what we do in this paper.

Step 6, Inscribed and Circumscribed Cases: In §7 we show that \mathcal{I}^* is foliated by invariant sets which (when completed) are holomorphically equivalent to the Riemann sphere. Under this equivalence, the map T_3 acts as a hyperbolic linear fractional transformation. The attracting fixed point in each level set is convex Poncelet and the repelling fixed point is the star-reordering of the attracting fixed point. This establishes Theorem 1.3 and all the statements of Theorem 1.2 pertaining to 8-gons in $\mathcal{I} \cup \mathcal{I}^*$.

3 Linear Independence

3.1 The Dependence Set

The vector fields X_1 and X_2 are linearly dependent on a certain set \mathcal{Y} defined by the following equations.

$$ac + bd + 1 = ac^2 + ca^2 + bd^2 + db^2 = 0. \quad (25)$$

I found this doing the analysis for Case 9 below. I don't have a geometric interpretation of \mathcal{Y} .

Lemma 3.1 F_1 and F_2 are never both positive on $\mathcal{Y} \cap \mathcal{X}$.

Proof: After a lot of trial and error I found the polynomial.

$$Y(x_1, x_2) = 512 + 216x_1x_2 + 192(x_1 + x_2) - 30(x_1 + x_2)^2 + (x_1 + x_2)^3. \quad (26)$$

We first show that $Y(F_1, F_2) = 0$ for in $\mathcal{Y} \cap \mathcal{X}$. Solving $ac + bd + 1 = 0$ we get $d = (-ac - 1)/b$. When we make this substitution we get the equation

$$Y(F_1(a, b, c, d), F_2(a, b, c, d)) = \frac{\phi_1\phi_2}{(abcd)^3}$$

where

$$\phi_1 = b^2(ac^2 + ca^2 + bd^2 + db^2)$$

and ϕ_2 is a messy polynomial we don't care about. Since $\phi_1 = 0$ on \mathcal{Y} and $abcd$ is nonzero on \mathcal{X} , we see that $Y(F_1, F_2) = 0$ on $\mathcal{Y} \cap \mathcal{X}$.

To finish the proof we just have to show that $Y(x_1, x_2) > 0$ when $x_1, x_2 > 0$. We compute that $\partial Y/\partial x_1 + \partial Y/\partial x_2 = 6(8 + x_1 + x_2)^2 > 0$. So, if this lemma is false, then Y is negative somewhere on the positive x -axis or on the positive y -axis. By symmetry it suffices to rule this out on the x -axis. We have $Y(x, 0) = (x + 2)(16 - x)^2 \geq 0$ on the positive x -axis. Hence $Y > 0$ when $x_1, x_2 > 0$. ♠

Lemma 3.1 implies that \mathcal{X}_+ is disjoint from \mathcal{Y} . The rest of the chapter is devoted to proving that that X_1 and X_2 are linearly independent everywhere on $\mathcal{X} - \mathcal{Y}$. This result combines with Lemma 3.1 to show that X_1 and X_2 are independent everywhere on \mathcal{X}_+

3.2 Resultants

The resultant of $P = a_2x^2 + a_1x + a_0$ and $Q = b_3x^3 + b_2x^2 + b_1x + b_0$ is the number

$$\text{res}(P, Q) = \det \begin{bmatrix} a_2 & a_1 & a_0 & 0 & 0 \\ 0 & a_2 & a_1 & a_0 & 0 \\ 0 & 0 & a_2 & a_1 & a_0 \\ b_3 & b_2 & b_1 & b_0 & 0 \\ 0 & b_3 & b_2 & b_1 & b_0 \end{bmatrix} \quad (27)$$

This vanishes if and only if P and Q have a common (complex) root. The case for general polynomials is similar; see §2 of [24].

In the multivariable case, one can treat two polynomials $P(x_1, \dots, x_n)$ and $Q(x_1, \dots, x_n)$ as elements of the ring $R[x_n]$ where $R = \mathbf{C}[x_1, \dots, x_{n-1}]$. The resultant $\text{res}_{x_n}(P, Q)$ computes the resultant in R and thus gives a polynomial in $\mathbf{C}[x_1, \dots, x_{n-1}]$. The polynomials P and Q simultaneously vanish at (x_1, \dots, x_n) only if $\text{res}_{x_n}(P, Q)$ vanishes at (x_1, \dots, x_{n-1}) .

3.3 The Proof modulo the Non-Vanishing Lemma

Let \mathcal{D} be the subset of \mathcal{X} where X_1 and X_2 are linearly dependent. We want to show that $\mathcal{D} = \mathcal{Y}$, the set defined by Equation 25. We compute that the following expression is an integer polynomial, and by definition it vanishes identically on \mathcal{D} .

$$f = \frac{abc^2d^2(X_{11}X_{22} - X_{21}X_{21})}{2(1-a+b)(1-b+a)(1-c+d)(1+c-d)}. \quad (28)$$

Here X_{ij} is the j th component of X_i .

A calculation – compare Lemma 2.4 – shows that $X_G \cdot \mu = 0$, where $\mu = (\alpha, -\alpha, -\beta, \beta)$ and

$$\alpha = ab(c+d)(1+c-d)(1+d-c), \quad \beta = cd(a+b)(1+a-b)(1+b-a).$$

When X_1 and X_2 are linearly dependent they are both multiples of X_G . Hence $X_1 \cdot \mu = X_2 \cdot \mu = 0$ on \mathcal{D} . We compute that

$$g = \frac{abcd(X_1 \cdot \mu)}{(1-a+b)(1-b+a)(1-c+d)(1+c-d)} \quad (29)$$

is an integer polynomial, and it vanishes identically on \mathcal{D} . We compute

$$h := \text{res}_a(f, g) = \phi_1\phi_2\phi_3\phi_4\phi_5^2\phi_6\phi_7^2\phi_8^2\phi_9. \quad (30)$$

Where ϕ_1, \dots, ϕ_9 are, in order, the functions

$$\begin{aligned} & b-1 \quad b+1 \quad b-c \quad b-d \quad c+d \quad bc+bd+cd-c^2 \\ & b-c+bc-bd-cd-c^2 \quad -b+c+bc-bd-cd-c^2 \quad c(bd^2+db^2)+(bd+1)(bd+1-c^2). \end{aligned} \quad (31)$$

One important point we note that is that the flow generated by X_G is a symplectomorphism which preserves F_1, F_2 . Hence \mathcal{D} is foliated by G -curves. We say ϕ_j is *bad* if it vanishes on a nontrivial arc of a G -curve that lies in $\mathcal{X} - \mathcal{Y}$, and otherwise *good*. Below we will prove:

Lemma 3.2 (Non-Vanishing) *The functions ϕ_1, \dots, ϕ_9 are all good.*

Since f and g vanish identically on \mathcal{D} , the resultant h also vanishes identically on points (b, c, d) such that $(a, b, c, d) \in \mathcal{D}$ for some choice of d . Suppose now that there exists a point $p \in \mathcal{D} - \mathcal{Y}$. Then there is an entire G -curve γ in $\mathcal{D} - \mathcal{Y}$. By the Non-Vanishing Lemma, each ϕ_j is nonzero on an open dense subset of γ . But then all ϕ_j are nonzero on the (open dense) intersection of these 9 open dense sets. In particular, we can find a point $(a, b, c, d) \in \mathcal{D}$ where $h(b, c, d) \neq 0$. This contradiction finishes the proof.

3.4 Proof of the Non-Vanishing Lemma

Given rational functions ψ_1 and ψ_2 we let ψ_1^* and ψ_2^* respectively be the numerator and denominator of ψ_1/ψ_2 when this is in lowest terms.

Cases 1 and 2: If $\phi_1 = b - 1$ is bad, then $b = 1$ and $X_2 \cdot (0, 1, 0, 0) = 0$. The only nonzero solution is

$$a = \frac{1 + c - d}{2c}. \quad (32)$$

We set a as in Equation 32 then compute that $\text{res}_c(f^*, g^*)$ and $\text{res}_d(f^*, g^*)$ are nontrivial 1-variable polynomials respectively in d and c . This means that f^* and g^* only vanish for finitely many pairs (c, d) . The ratios f/f^* and g/g^* have the form $c^i(1 + c - d)^j$ and do not vanish. Hence f and g only vanish at finitely many points in \mathcal{X} with $b = 1$ and a as in Equation 32. This is a contradiction. Hence ϕ_1 is good. ϕ_2 is good by symmetry: The map $p \rightarrow -p$ carries ϕ_1 to ϕ_2 and preserves $\mathcal{D}, \mathcal{X}, \mathcal{Y}$.

case 3: Suppose that $\phi_3 = b - c$ is bad. Then we have $b = c$ and

$$X_G \cdot (0, 1, -1, 0) = 4(a + d)(a - d) = 0.$$

Hence $a = \pm d$. In either case we compute $G(a, b, b, \pm a) = 0$ so our point does not lie in \mathcal{X} . This contradiction shows that ϕ_3 is good.

Case 4: Suppose $\phi_4 = b - d$ is bad. We have $d = b$ and

$$0 = X_G \cdot (0, 1, 0, -1) = \frac{4(a-c)(a-b+c)(ac+b^2-1)}{ac}$$

If $a = c$ then $(a, b, a, b) \notin \mathcal{X}$. If $a = (1 - b^2)/c$ we compute $G(a, b, c, b) = 0$. Again, our point does not lie in \mathcal{X} . Hence $a = b - c$. The rest of the proof is like Case 1 except that we use the b and c variables for the resultants. This time f/f^* and g/g^* both have the form $b^i(b - 2c)^j$ and these do not vanish, because $b = 2c$ leads to a point $(c, 2c, c, 2c) \notin \mathcal{X}$. Hence ϕ_4 is good.

Case 5: Suppose $\phi_5 = c + d = 0$. Then $d = -c$. We first compute

$$0 = g(a, b, c, -c) = c^4(1 - a + b)(1 + a - b)(a + b)^2. \quad (33)$$

The first 3 factors are nonzero on \mathcal{X} . Hence $b = -a$. When $d = -c$ and $b = -a$ we solve $X_{11}X_{23} - X_{13}X_{21} = 0$ and find that

$$a = c, \quad \text{or} \quad a = \frac{-1}{2c}, \quad \text{or} \quad a = \frac{c}{2c-1} \quad \text{or} \quad a = \frac{-c}{2c+1}. \quad (34)$$

Choice 1 gives $(a, -a, a, -a) \notin \mathcal{X}$. Choice 2 gives a point in \mathcal{Y} . Choices 3 and 4 respectively lead to $F_1 = 0$ and $F_2 = 0$. Hence ϕ_5 is good.

Case 6: Suppose ϕ_6 is bad. Setting $\phi_6 = 0$, making the substitution for b , then setting $X_G \cdot \nabla \phi_6 = 0$, we get

$$b = \frac{c^2 - cd}{c + d}, \quad a = \frac{c^2 - cd}{c + d} \quad \text{or} \quad a = \frac{-2c - c^2d + d^3}{(c + d)^2}.$$

Since ϕ_5 is good, we can perturb along our G -curve to that $c + d \neq 0$ and all our substitutions are well defined. There are 2 choices for a . The first choice leads to $G(a, b, c, d) = 0$, so the second choice obtains. The rest of the proof is like Case 1 except now f/f^* and g/g^* have the form $c^i(c + d)^j$ and this expression is good by Case 5. Hence ϕ_6 is good.

Cases 7 and 8: Suppose $\phi_7 = 0$. Solving for b we have

$$b = \frac{c(1 + c + d)}{1 + c - d}. \quad (35)$$

Solving $X_G \cdot \nabla \phi_7 = 0$ for a yields

$$a = \frac{d - cd - d^2}{1 + c - d} \text{ or } \frac{d + 5cd + 7c^2d + 3c^3d + 4c^2d^2 - d^3 + cd^3}{-1 - c + c^2 + c^3 - 2d - 6cd - 4c^2d + d^2 + cd^2 + 2d^3}. \quad (36)$$

The first choice leads to $F_2(a, b, c, d) = 0$ and this point does not lie in \mathcal{X} . Hence a is the second choice. The rest of the proof is as in Step 1, but

$$\frac{f}{f^*} = \frac{g}{g^*} = \frac{c^2(a + ac - d - ac + cd + d^2)}{(1 + c - d)^4}.$$

The factors c and $(1 + c - d)$ do not vanish in \mathcal{X} . The big factor on the right does not vanish because it is also a factor of $F_2(a, b, c, d) \neq 0$. Hence ϕ_7 is good. ϕ_8 is good by symmetry.

Case 9: Suppose that ϕ_9 is bad. Solving $\phi(a, b, c, d) = 0$ for c we get a quadratic equation. The two roots c_1 and c_2 satisfy

$$c_1 + c_2 = \frac{bd^2 + db^2}{bd + 1}, \quad c_1c_2 = -1 - bd. \quad (37)$$

The permutation $\pi(a, b, c, d) = (c, d, a, b)$ preserves \mathcal{D} . The same arguments as above, with the coordinates permuted, show that $\phi_j \circ \pi$ is good for $j = 1, \dots, 8$. Only the badness of $\phi_9 \circ \pi$ can cause $(c, d, a, b) \in \mathcal{D}$. Hence $\phi_9(c, d, a, b) = 0$. Solving $\phi(c, d, a, b) = 0$ for a we get the same result as in Equation 37. In other words, $a, c \in \{c_1, c_2\}$.

The function $\phi_4 \circ \pi = a - c$ is good, so a and c are the *two different solutions* of Equation 37. We set $c = c_1$ and $a = c_2$. Hence $ac + bd + 1 = 0$. This is the first defining relation for \mathcal{Y} . As an aside, we have $bd + 1 \neq 0$ because $ac \neq 0$. We also now have

$$a + c = \frac{bd^2 + db^2}{bd + 1} = \frac{bd^2 + db^2}{-ac},$$

which implies that $ac^2 + ca^2 + bd^2 + db^2 = 0$. This is the second defining relation for \mathcal{Y} . Hence $(a, b, c, d) \in \mathcal{Y}$, a contradiction. Hence ϕ_9 is good.

4 Cylinders in the Positive Part

4.1 Overview

We carry out Step 2 of the outline given §2.8. Recall that \mathcal{X}_+ is the subset of \mathcal{X} where all the factors of F_1 , F_2 , and G are positive. We also throw out points of the form (a, b, a, b) . Let L_+ be a level set of \mathcal{X}_+ . Recall that a G -curve of L_+ is one that is integral to X_G . Let \mathcal{U} be the set (a, b, c, d) with $\max(a + b, c + d) = 1$. Here is an outline of what we do in this chapter.

1. In §4.2 we prove the L_+ is bounded in \mathbf{R}^4 .
2. In §4.3 we classify the accumulation points of L_+ in $\mathbf{R}^4 - \mathcal{X}_+$.
3. In §4.4 we combine a monotonicity idea related to Lemma 2.4 with the classification from §4.3 to prove that each G -curve intersects \mathcal{U} exactly once. We use this property to prove that \mathcal{X}_+ is path connected.
4. In §4.5 we show that $L_+ \cap \mathcal{U}$ is a finite union of closed loops. We then use a homotopy argument to that in fact $L_+ \cap \mathcal{U}$ is just the nice loop from Step 2. The key idea is that because *every single level set* is smooth and the relevant intersections with \mathcal{U} are compact, there is no way for the topology to change as we move around in \mathcal{X}_+ .

Since L_+ is foliated by G -curves, each of which intersects \mathcal{U} once, we see that L_+ is homeomorphic to the product of an open interval with the loop $L_+ \cap \mathcal{U}$. Hence L_+ is a cylinder.

4.2 Boundedness of the Level Sets

Lemma 4.1 *The level set L_+ is bounded in \mathbf{R}^4 .*

Proof: We work with the functions g_{ab} and g_{cd} from Equation 6.

$$g_{ab} = \frac{1 - a^2 - b^2}{ab}, \quad g_{cd} = \frac{1 - c^2 - d^2}{cd}.$$

Suppose $\{(a_n, b_n, c_n, d_n)\}$ is an unbounded sequence in L_+ . It suffices to suppose one of c_n or d_n tends to ∞ . Since $|c_n - d_n| < 1$, both of these coordinates tend to ∞ . Hence $g_{cd} \rightarrow -2$. We will show that $g_{ab} \rightarrow +2$ as $n \rightarrow \infty$. This gives $|g_{ab} + g_{cd}| \rightarrow 0$ as $n \rightarrow \infty$. Since $|g_{ab}^* + g_{cd}^*| \leq 2$, we get $G(a_n, b_n, c_n, d_n) \rightarrow 0$ on the level set, a contradiction

Passing to a subsequence we can assume that $a_n + b_n > 1$ for all n or $a_n + b_n < 1$ for all n . In the first case $g_{ab} < 2$. Since $g_{ab} + g_{cd} > 0$ and $g_{cd} \rightarrow -2$ we must have $g_{ab} \rightarrow 2$. Now suppose $a_n + b_n < 1$ for all n .

Look at the factor $a - d + ac + bd > 0$ of F_2 and note that $c_n < d_n + 1$:

$$\begin{aligned} 0 < a_n - d_n + a_n c_n + b_n d_n < a_n - d_n + a_n(d_n + 1) + b_n d_n = \\ 2a_n + (a_n + b_n - 1)d_n &= (-d_n + b_n d_n) + (a_n d_n + 2a_n). \end{aligned} \quad (38)$$

Since $d_n \rightarrow +\infty$, Equation 38 implies that $a_n + b_n \rightarrow 1$.

If a_n, b_n remain in a compact subset of $(0, 1)$ we have $g_{ab} \rightarrow 2$. We just have to worry about the case that $(a_n, b_n) \rightarrow (1, 0)$ or $(0, 1)$. We will consider the second case. The first case has a similar treatment, except that we would re-do Equation 38 with the factor $b - c + ac + bd > 0$ of F_1 .

Divide the last expression of Equation 38 by $a_n d_n$ and rearrange to get:

$$\frac{1 - b_n}{a_n} < 1 + \epsilon, \quad \epsilon = \frac{2}{d_n}.$$

Since $d_n \rightarrow \infty$ we can take $\epsilon > 0$ as small as we like. But then

$$\frac{1 - a_n^2 - b_n^2}{a_n b_n} < \frac{1 - b_n^2}{a_n b_n} = \frac{1 + b_n}{b_n} \times \frac{1 - b_n}{a_n} < \left(1 + \frac{1}{b_n}\right) \times (1 + \epsilon). \quad (39)$$

Since $b_n \rightarrow 1$, Equation 39 says that $\limsup(g_{ab}) \leq 2$. Since $g_{ab} + g_{cd} > 0$ and $g_{cd} \rightarrow -2$ we also have $\liminf g_{ab} \geq 2$. Hence $g_{ab} \rightarrow 2$. ♠

4.3 Classification of the Accumulation Points

Lemma 4.2 *Up to the permutation I from §5, every accumulation point of L_+ not in \mathcal{X} has the following form.*

1. $(0, \bar{b}, \bar{b}, 0)$ for $\bar{b} \in [0, 1)$.
2. $(0, 1, 1, 0)$ or $(0, 1, 0, 1)$ or $(1, 0, 1, 0)$.
3. $(0, 1, \bar{c}, \bar{d})$ or $(1, 0, \bar{c}, \bar{d})$ for $\bar{c} > 0$ and $\bar{d} > 0$ and $\bar{c} + \bar{d} > 1$.

Proof: Consider a sequence $\{(a_n, b_n, c_n, d_n)\} \in L_+$ converging to some $(\bar{a}, \bar{b}, \bar{c}, \bar{d}) \in \mathbf{R}^4 - L_+$. If $\bar{a}, \bar{b}, \bar{c}, \bar{d} > 0$ then some factor of the numerator of F_1 or F_2 vanishes at our limit point. But then the function F_1 or F_2 also vanishes there. This contradicts the fact that F_1 and F_j are constant on L_+ . Hence, at least one of the limit coordinates is 0.

The rest of our proof only uses the fact that $|G|$ is bounded on L_+ . Since we don't care about the sign of G , we can freely use the symmetries I and J from Equation 5 to simplify our work. (Composition with J switches F_1 and F_2 and negates G .) Using I and J we can assume that $\bar{a} = 0$. Since $|a - b| \leq 1$ when all factors of F_1 and F_2 are positive, we have $\bar{b} \in [0, 1]$.

We use \sim to denote the relation that the ratio of two quantities is asymptotically 1 as $n \rightarrow \infty$. We write

$$b_n = 1 - K_n a_n.$$

Let NF_j and DF_j respectively denote the numerator and denominator of F_j . We have

$$\lim \frac{DF_j(a_n, b_n, c_n, d_n)}{a_n} = \bar{b}\bar{c}\bar{d}.$$

Let F_{jkn} denote the k th factor of $NF_j(a_n, b_n, c_n, d_n)$. The trick in our proof is finding the right factor of NF_j to divide by a_n . We find that

$$\begin{aligned} \frac{F_{11n}}{s_n} &\sim 1 + K_n, & F_{12n} &\rightarrow 1 + \bar{c} - \bar{d}, & F_{13n} &\rightarrow 1 - \bar{c} + \bar{d}, & F_{14n} &\rightarrow 2\bar{d}. \\ F_{21n} &\rightarrow 2, & F_{22n} &\rightarrow 1 - \bar{c} + \bar{d}, & F_{23n} &\rightarrow \bar{c} + \bar{d} - 1, & \frac{F_{24n}}{a_n} &\sim 1 + \bar{c} - K_n\bar{d}. \end{aligned} \quad (40)$$

We now distinguish 3 cases:

Case 1: Suppose $\bar{b} < 1$. Then $K_n \rightarrow +\infty$. Since $a_n^{-1}F_{24n} > 0$ we have $\bar{d} = 0$. Since $c > 0$ and $d > 0$ and $|c - d| < 1$ we have $g_{cd} > -2$. Since $\bar{b} < 1$ and $\bar{a} \rightarrow 0$ we have $g_{ab} \rightarrow \infty$. Hence $g_{ab} + g_{cd} \rightarrow +\infty$ and (given that $|G|$ is bounded) also $g_{ab}^* + g_{cd}^* = a - b + c - d \rightarrow 0$. Hence $t = 0$. This gives us $(0, \bar{b}, \bar{b}, 0)$ as the limit.

Case 2: Suppose that $\bar{b} = 1$ and $\bar{c}\bar{d} = 0$. Since $|c_n - d_n| < 1$ we have $\bar{c} + \bar{d} \leq 1$. The positivity and asymptotics of F_{23n} gives $\bar{c} + \bar{d} \geq 1$. Hence $\bar{c} + \bar{d} = 1$. The only choices are $(\bar{c}, \bar{d}) = (1, 0)$ or $(0, 1)$.

Case 3: Suppose $\bar{b} = 1$ and $\bar{c}\bar{d} > 0$. As in Case 2, the positivity and asymptotics of F_{23n} implies that $\bar{c} + \bar{d} \geq 1$. We will assume that $\bar{c} + \bar{d} = 1$ and derive a contradiction. Since $\bar{c}\bar{d} > 0$ we have $|\bar{c} - \bar{d}| < 1$. But then the last 3 factors in the first row of Equation 40 are positive. This forces $\{K_n\}$ to be bounded. But then $\{a_n^{-1}F_{24n}\}$ is bounded. Since $\bar{c} + \bar{d} - 1 = 0$, we see that $F_{23n} \rightarrow 0$. Hence $F_2 \rightarrow 0$. But F_2 is bounded away from 0 (and indeed constant) on our sequence. This is a contradiction. Hence $\bar{c} + \bar{d} > 1$. ♠

4.4 Analysis of Flowlines

Let χ be a G -curve in L_+ . We orient χ so that its tangent vectors are positive multiples of X_G . As we remarked after Lemma 2.4, both ends of χ exit every compact subset of \mathcal{X}_+ . Hence, both ends have at least one accumulation point.

Lemma 4.3 *The backwards end of any G -curve has a unique accumulation point, and it has the form $(x, 0, 0, x)$ or $(0, x, x, 0)$ for some $x \in [0, 1]$. The forwards end of any G -curve has a unique accumulation point, and it is either $(1, 0, 1, 0)$ or $(1, 0, x, y)$ or $(x, y, 1, 0)$ with $x, y > 0$ and $x + y > 1$.*

Proof: Thanks to Equations 18 – 22, the functions g_{ab} and g_{cd} and g_{ab}^* and g_{cd}^* are all monotone along χ . In particular, $a - b$ and $c - d$ are increasing as we move forward along χ .

Suppose that the backwards end of χ accumulates on $(1, 0, x, y)$. But $a - b$ increases along χ and remains less than 1. This is an immediate contradiction. The same argument, using $c - d$ in place of $a - b$, rules out and $(x, y, 1, 0)$. Suppose $(0, 1, x, y)$ is a backwards accumulation point. Since we have the inequality $a - b + c - d > 0$ in \mathcal{X}_+ we must have $x - y \geq 1$. But, again, this contradicts the fact that $c - d$ increases along χ and always satisfies $c - d < 1$. The same argument rules out $(x, y, 0, 1)$ as a limit point. Lemma 4.2 now says that any accumulation point has the claimed form.

The uniqueness follows from the characterization of the backwards accumulation points and from the monotonicity of $a - b$ and $c - d$ along χ . One final observation. Given the nature of the backwards limit point, the quantity $a - b + c - d$ converges to 0 at the backwards end of χ .

Suppose that the forward end of χ accumulates on $(a', 0, 0, a')$. Then the quantity $a - b + c - d$ converges to 0 in the forward direction along χ . Given the monotonicity of $a - b + c - d$, this is only possible if $a - b + c - d = 0$ along χ , a contradiction. The same argument rules out a forward limit of $(0, b', b', 0)$. Another monotonicity argument, as in the backwards case, rules out forward limit points of the form $(0, 1, x, y)$ and $(x, y, 0, 1)$. The only choices left are the ones advertised in the statement of this lemma.

For forward uniqueness, note that g_{ab} and g_{cd} (being monotone increasing and bounded from above by 2) and g_{ab}^* and g_{cd}^* (being monotone decreasing and bounded from below by -2) have forward limits along χ . These limits uniquely specify $(1, 0, x, y)$ or $(x, y, 1, 0)$. If *both* $(1, 0, x, y)$ and $(x, y, 1, 0)$ are forward limits, then χ bounces back and forth repeatedly while exiting every compact subset of \mathcal{X}_+ , forcing an impossible continuum of limit points. ♠

Lemma 4.4 *Each G -curve in L_+ intersects \mathcal{U} exactly once.*

Proof: Let χ be a G -curve. Let us take care of the uniqueness first. When $a, b > 0$, a condition we have on χ , we have $g_{ab} > 2$ if and only if $a + b < 1$. Also, $g_{ab} = 2$ if and only if $a + b = 1$. Since g_{ab} strictly decreases along χ , we have $g_{ab} = 2$ only once. Likewise we can have $g_{cd} = 2$ only once. Hence we can have $\max(g_{ab}, g_{cd}) = 2$ only once.

Now we turn to the existence of the intersection. The backwards limit point of χ has the form (a, b, c, d) where $\max(a + b, c + d) < 1$. The forwards limit point has the form (a, b, c, d) where $\max(a + b, c + d) \geq 1$ and we have equality only if the forwards limit point is $(1, 0, 1, 0)$. So, our proof is done unless the forward limit point is $(1, 0, 1, 0)$. We consider this case.

Let $\{a_n, b_n, c_n, d_n\}$ be a sequence along χ converging to $(1, 0, 1, 0)$. All our proof uses is that the sequences $\{F_n(a_n, b_n, c_n, d_n)\}$ are bounded away from 0. It suffices to show there is some n such that $\max(a_n + b_n, c_n + d_n) > 1$. We assume not and derive a contradiction. We write $a_n = 1 - b_n - h_n$ and $c_n = 1 - d_n - k_n$ with $b_n, d_n, h_n, k_n \geq 0$ and $b_n, d_n, h_n, k_n \rightarrow 0$. We have

$$F_1 = \frac{1}{a_n c_n} \times (2 - 2b_n - h_n) \times (2 - 2d_n - k_n) \times$$

$$\frac{2b_n d_n + b_n k_n - (1 - d_n - k_n)h_n}{b_n} \times \frac{2b_n d_n + d_n h_n - (1 + b_n + h_n)k_n}{d_n} <$$

$$3 \times 2 \times 2 \times (2d_n + k_n) \times (2b_n + h_n) \rightarrow 0.$$

Hence $F_1 \rightarrow 0$ on L_+ , a contradiction. ♠

Lemma 4.5 *The space \mathcal{X}_+ is path connected.*

Proof: By Lemma 4.4, every point of \mathcal{X}_+ can be joined to $\mathcal{X}_+ \cap \mathcal{U}$ by a G -curve. So, we just have to prove that $\mathcal{X}_+ \cap \mathcal{U}$ is path connected.

Let $\mathcal{U}_{abcd} = \mathcal{U}_{ab} \cap \mathcal{U}_{cd}$. Now we show that we can join any point of $\mathcal{X}_+ \cap \mathcal{U}_{ab}$ to a point of $\mathcal{X}_+ \cap \mathcal{U}_{abcd}$ by a path that remains in \mathcal{X}_+ . The same argument works with (c, d) replacing (a, b) .

Choose $(a, b, c, d) \in \mathcal{X}_+ \cap \mathcal{U}_{ab}$. This point satisfies $a + b = 1$ and $c + d < 1$. We connect our point to a nearby point (a', b', c', d') where $a' - b' \neq c' - d'$. So, without loss of generality assume that $a - b \neq c - d$. Consider the segment σ given by $(a, b, c, d) \rightarrow (a, b, c + t, d + t)$. We start at $t = 0$ and we end when we reach \mathcal{U}_{abcd} . Along σ we have $g_{ab}, g_{cd} \geq 2$ so $g_{ab} + g_{cd} \geq 4$.

The function $g_{ab}^* + g_{cd}^*$ is constant along σ . Hence the factors of G remain positive along σ . Consider the factors of F_1 and F_2 . First, a, b, c, d all remain positive along σ . The factors of the form $1 + \mu - \nu$ are constant along σ . A typical one is $1 - c + d$. Consider a factor of the form $\zeta = e + \mu - \nu$ with $e = ac + bd$ and $\mu \in \{\pm a, \pm b\}$ and $\nu \in \{\pm c, \pm d\}$. Along σ we have $de/dt = 1$ and $d\mu/dt = 0$ and $d\nu/dt = \pm t$. We conclude that $d\zeta/dt \geq 0$. Hence all factors of F_1 and F_2 remain positive on σ . Finally, thanks to our initial perturbation, the endpoint of σ does not have the form (a, b, a, b) .

In \mathcal{U}_{abcd} we have $b = 1 - a$ and $d = 1 - c$. Let λ be the line $a = c$. Let τ be the open triangle $(a, 1 - a, c, 1 - c)$ with $a, c, 1 - a, 1 - c, a + c - 1 > 0$. We have $\mathcal{X}_+ = \mathcal{U}_{abcd} = \tau - \lambda$. The space $\tau - \lambda$ has 2 components. To finish the proof we just have to connect any point in one component to any point in the other using a path in \mathcal{X}_+ . We start with the point $(3/4, 1/4, 2/3, 1/3) \in \tau - \lambda$ and move linearly to $(3/4, 1/3, 2/3, 1/4)$. Then we move linearly to $(2/3, 1/3, 3/4, 1/4) \in \tau - \lambda$. One can easily check that this bigon remains in \mathcal{X}_+ . ♠

4.5 A Closer Look at the Intersection

Lemma 4.6 $L_+ \cap \mathcal{U}$ is compact.

Proof: We will suppose this is false and then derive a contradiction. Let $\{a_n, b_n, c_n, d_n\} \in L_+$ be a sequence of points which exits every compact subset of \mathcal{U} . Since \mathcal{U} is defined by a closed condition, our sequence must exit every compact subset of \mathcal{X}_+ . Without loss of generality assume that $a_n + b_n = 1$ and $c_n + d_n \leq 1$. By Lemma 4.2 there are 4 possible accumulation points: $(0, 1, 0, 1)$ or $(1, 0, 1, 0)$ or $(1, 0, 0, 1)$ or $(0, 1, 1, 0)$. The limit $(0, 1, 0, 1)$ cannot occur because we need $a - b + c - d > 0$. The proof of Lemma 4.4 rules out $(1, 0, 1, 0)$. The symmetry J swaps the remaining cases, and our last arguments never uses G . So, it suffices to treat the case of $(0, 1, 1, 0)$.

We set $b_n = 1 - a_n$ and $c_n = 1 - d_n - h_n$. We have $a_n, c_n, h_n \rightarrow 0$ and all these are positive. Remembering that F_1 is constant on L_+ , we compute

$$F_1 = \frac{1}{b_n c_n} \times \frac{2a_n}{a_n} \times (2 - 2d_n - h_n) \times (1 - a_n)(2d_n + h_n) \times \frac{2d_n - 2a_n d_n - a_n h_n}{d_n} \leq$$

$$3 \times 2 \times 2 \times (2d_n + h_n) \times 2 \rightarrow 0.$$

Hence $F_1 = 0$ on L_+ , a contradiction. ♠

Lemma 4.7 L_+ is transverse to \mathcal{U}_{ab} and to \mathcal{U}_{cd}

Proof: By symmetry it suffices to consider \mathcal{U}_{ab} . Since L_+ is smooth it suffices to prove that X_G is not tangent to \mathcal{U}_{ab} . The vector $(1, 1, 0, 0)$ is perpendicular to this space, and (setting $b = 1 - a$) we compute

$$X_G \cdot (1, 1, 0, 0) = \frac{4a(1-a)(1+c-d)(1-c+d)}{cd} \neq 0. \quad (41)$$

This does it. ♠

By transversality and compactness, the intersection $L_+ \cap \mathcal{U}$ is a smooth 1-manifold away from \mathcal{U}_{abcd} and overall a compact topological 1-manifold. A smooth arc which starts in \mathcal{U}_{ab} and hits \mathcal{U}_{abcd} simply continues across the intersection into \mathcal{U}_{cd} as another smooth arc. There is one fine point here. Why couldn't two loops exactly touch along \mathcal{U}_{abcd} , making a figure 8? In this case, we could look at the union of G -curves through this figure 8 and we would get the product of a figure 8 and an arc. This is not a surface, which contradicts the fact that L_+ is a smooth surface. In short $L_+ \cap \mathcal{U}$ is a finite union of $C(L_+)$ closed loops. Recall that such a loop is nice if it intersects \mathcal{U}_{abcd} . Let $N(L_+) \leq C(L_+)$ denote the number of nice loops.

Lemma 4.8 Both $C(L_+)$ and $N(L_+)$ are independent of L_+ .

Proof: Consider $C(\cdot)$ first. Imagine that we have a closed arc in \mathcal{X}_+ . We think of $C(\cdot)$ as a function on this arc. Since every single intersection $L_+ \cap \mathcal{U}$ is a closed topological 1-manifold, the various loops cannot merge or split into two as we go along the arc. Also, by compactness, none of the loops can exit all compact subsets of \mathcal{U} . Finally, no loop can shrink to a point. We conclude that $C(\cdot)$ is constant along our arc. Since \mathcal{X}_+ is path connected, we see that $C(\cdot)$ is globally constant. The argument for $N(\cdot)$ is the same. ♠

Lemma 4.9 $N(L_+) = 1$.

Proof: Set $x^* = 1 - x$. At the point (a, a^*, c, c^*) we have $F_1 = 16a^*c^*$ and $F_2 = 16ac$. There are at most 2 values of (a, c) which gives any particular choice (F_1, F_2) . The number of these solutions is twice $N(L_+)$ because each nice loop hits \mathcal{U}_{abcd} twice. We conclude that $N(L_+) \leq 1$. At the same time, we have $N(L_+) \geq 1$ because some level sets obviously intersect \mathcal{U}_{abcd} . The two bounds give $N(L_+) = 1$. ♠

Lemma 4.10 $C(L_+) = 1$.

Proof: The space $\mathcal{X}_+ \cap \mathcal{U}$ is foliated by its intersection with the level sets, and each intersection is a finite number of loops. Call a point in $\mathcal{X}_+ \cap \mathcal{U}$ *happy* if it lies on a nice loop and otherwise *unhappy*. It suffices to prove that all points are happy.

By compactness of the intersections, and continuity of the intersections, the set of happy points is closed. We claim that the set of unhappy points is also closed. Assuming this claim, and the fact that $\mathcal{U} \cap \mathcal{X}_+$ is path connected, we see that either all points are happy or all points are unhappy. Since some points are happy, all points are happy.

If our claim is false then we can find a sequence $\{\gamma_n\}$ of loops which avoid \mathcal{U}_{abcd} , which remain in a compact subset of $\mathcal{U} \cap \mathcal{X}_+$, and which touch \mathcal{U}_{abcd} in the limit. Each of our loops lies in one of \mathcal{U}_{ab} or \mathcal{U}_{cd} . This means that the limit loop γ only touches \mathcal{U}_{abcd} in a single point. But then $\gamma \cap I(\gamma)$ are a pair of loops making a figure 8. This is something we have already discussed and ruled out. This proves the claim. ♠

Now we know that $L_+ \cap \mathcal{U}$ is a single nice loop. Hence L_+ is an open cylinder. This completes our proof.

Remark:

As a byproduct of our proof, we see that every level set of \mathcal{X}_+ contains exactly 2 points of the form (a, a^*, c, c^*) . Again $x^* = 1 - x$. From this we see that $F_1, F_2, G \in (0, 16)$ on \mathcal{X}_+ . I discovered this last fact numerically but couldn't find a purely algebraic proof.

5 Intrinsic Boundedness and Concavity

5.1 Overview

We carry out Step 3 of the outline in §2.8. We show that each level set L_+ of \mathcal{X}_+ is intrinsically bounded, and has ends (i.e. metric completions) which are locally concave everywhere except 2 points. Let Δ be as in Equation 4. Let $\iota_5 = A\delta A\delta A$. Both these maps are isometric involutions with respect to any flat metric on L_+ coming from the integrable structure.

Let L'_+ denote the subset of L_+ consisting of points (a, b, c, d) with $\max(a + b, c + d) < 1$. Note that L'_+ is foliated by G -arcs which connect the back end of L_+ to the nice loop. In particular, L'_+ is a sub-cylinder of L_+ . In §5.2 we prove two results:

1. $\Delta(L_+) = L_+$ and Δ swaps the ends of L_+ .
2. $\iota_5(L'_+) = L'_+$ and ι_5 swaps the ends of L'_+ .

What makes this powerful is that the front end of L'_+ , namely the nice loop, lies in \mathcal{X}_+ , and we can make direct calculations on it. Using the (intrinsic) isometry ι_5 we transfer metric info about the front end of L'_+ to the back end of L_+ . Using Δ we can then transfer metric info about the back end of L_+ to metric info about the front end of L_+ . We will use this technique in §5.3 to prove the intrinsic boundedness result and in §5.4 to prove the concavity result. Finally in §5.5 we further discuss the nature of the corners of L_+ .

5.2 Reversal Lemmas

Lemma 5.1 (Reversal I) $\Delta(L_+) = L_+$ and Δ swaps the ends of L_+ .

Proof: We already know that \mathcal{X}_+ is path connected. A single evaluation, say for the point $(1/4)(2, 1, 2, 1)$, suffices to show that $\Delta(\mathcal{X}_+) \cap \mathcal{X}_+ \neq \emptyset$. Since the component functions of Δ are positive and since $F_j \circ \Delta = F_j$ and $G \circ \Delta = G$ we see that Δ cannot map any point of \mathcal{X}_+ into the boundary of \mathcal{X}_+ . This would cause some invariant to vanish. Since \mathcal{X}_+ is connected, this implies that $\Delta(\mathcal{X}_+) \subset \mathcal{X}_+$. Since Δ is an involution we have $\Delta(\mathcal{X}_+) = \mathcal{X}_+$. Since Δ preserves both invariants we must have $\Delta(L_+) = L_+$. Since Δ preserves both invariants and negates the symplectic form, we see that Δ is an isometry of L_+ which reverses the direction of the G -curves. Hence Δ swaps the ends of L_+ . ♠

Let L'_+ denote the subset of L_+ consisting of arcs of G -curves which join points on the nice loop $L_+ \cap \mathcal{U}$ to the backwards end of L_+ . This definition makes sense because each G -curve intersects the nice loop once.

Lemma 5.2 (Reversal II) $\iota_5(L'_+) = L'_+$ and ι_5 swaps the ends of L'_+ .

The rest of this section is devoted to proving this result.

Lemma 5.3 For any $p \in L_+ \cap \mathcal{U}$ we have $\iota_5(p) = (0, x, x, 0)$ or $(x, 0, 0, x)$.

Proof: Recall that \mathcal{U}_{ab} consists of points (a, b, c, d) with $a + b = 1$ and $c + d \leq 1$. For $(a, 1 - a, c, d) \in L_+$ we compute

$$\iota_5(a, 1 - a, c, d) = (0, x, x, 0), \quad \beta = \frac{1 - (c + d)}{(c + d) - (c - d)^2}. \quad (42)$$

A similar calculation works for points in \mathcal{U}_{cd} and there we get $(x, 0, 0, x)$. ♠

Lemma 5.4 The map ι_5 is well-defined and real analytic in the cube $(0, 1)^4$. If $(a', b', c', d') = \iota_5(a, b, c, d)$ and $(a, b, c, d) \in L'_+$ then $(a', d') \neq (0, 0)$ and $(b', c') \neq (0, 0)$.

Proof: Let $x^* = 1 - x$. The denominator of each coordinate equals one of two products:

$$(b + c - ac - bd)\mu, \quad (a + d - ac - bd)\mu,$$

$$\mu = aca^*c^* + bdb^*d^* + abcc^* + abdd^* + cdaa^* + cdbb^* + 2abcd.$$

These do not vanish on $(0, 1)^4$ and so ι_5 is well-defined and real analytic.

When we solve $a' = d' = 0$ we find that either $cd = 0$ or $a + b = 1$ or

$$a = \frac{d(1 + c - d)}{1 - (c + d)}, \quad b = \frac{c(1 - c + d)}{1 - (c + d)}. \quad (43)$$

The first case gives points not in \mathcal{X}_+ . The second case gives points not in L'_+ . In the third case, Equation 43 leads to $a - b + c - d = 0$, so that $(a, b, c, d) \notin \mathcal{X}_+$. Hence $(a, d') \neq (0, 0)$. The same argument works for (b', c') and this also follows from symmetry. ♠

Let \mathcal{X}'_+ denote the subset of \mathcal{X}_+ consisting of those points (a, b, c, d) with $a + b < 1$ and $c + d < 1$. Call a point $p \in \mathcal{X}'_+$ *good* if $\iota_5(p) \in \mathcal{X}'_+$. The set of good points is non-empty. For instance, $p = (1/2, 2/3, 2/3, 1/4)$ is good. By Lemma 5.4, the set of good points is open.

Lemma 5.5 *The set of good points is closed.*

Proof: Let $p = \lim p_n$ be the limit of a sequence of good points. By Lemma 5.4, the point $q = \iota_5(p)$ is well-defined, and the limit of a sequence of points $\{q_n\}$ where $q_n = \iota_5(p_n)$. We suppose p is not good and we derive a contradiction. We know that $q \notin \mathcal{X}'_+$. If $q \in \mathcal{X}_+$ then we must have $q \in \mathcal{U}$. But then, since ι_5 is an involution, Lemma 5.4 implies that $p = \iota_5(q)$. But this contradicts Lemma 5.3. Hence $q \in \mathbf{R}^4 - \mathcal{X}_+$.

In our proof of Lemma 4.3 we did not really use the fact that we were taking accumulation points of a single level set. The proof there just requires that the sequences $\{F_j(a_n, b_n, c_n, d_n)\}$ are bounded away from 0. Hence q has the form given in the conclusion of Lemma 4.3. Lemma 5.4 rules out $q = (0, x, x, 0)$ or $q = (x, 0, 0, x)$. Since q is the limit of points with $\max(a_n + b_n, c_n + d_n) < 1$ we cannot have $q = (1, 0, x, y)$ etc. with $x + y > 1$. The only cases are $q = (1, 0, 1, 0)$ or $q = (0, 1, 0, 1)$. Since $G(q_n) > 0$ we cannot have $q = (0, 1, 0, 1)$. If $q = (1, 0, 1, 0)$ then having $q_n \rightarrow q$ violates the proof of Lemma 4.4 because $\{F_j(q_n)\}$ is bounded away from 0 for $j = 1, 2$. ♠

The same proof that \mathcal{X}_+ is path connected shows that \mathcal{X}'_+ is path connected. (We join every point of \mathcal{X}'_+ to a point of $\mathcal{U} \cap \mathcal{X}_+$ by a G -curve and then the proof is the same.) Since the subset of good points is non-empty, open, and closed, all points are good. Hence $\iota_5(\mathcal{X}'_+) \subset \mathcal{X}'_+$. Since ι_5 is an involution, we have $\iota_5(\mathcal{X}'_+) = \mathcal{X}'_+$. Since $F_j \circ \iota_5 = F_j$ we see that $\iota_5(L'_+) = L'_+$ for all level sets L_+ of \mathcal{X}_+ . Finally ι_5 negates the symplectic form and preserves the invariants. Hence ι_5 reverses the direction of the G -curves in L'_+ . Hence ι_5 swaps the ends of L'_+ . We could also deduce this from Equation 42. This completes the proof of the Reversal Lemma II.

5.3 Intrinsic Boundedness

We choose a flat metric on L_+ coming from the integrable structure. The result is independent of choice. By compactness, every point of $p \in L_+$ is (intrinsically) less than D_p units from every point of $L_+ \cap \mathcal{U}$ for some constant D_p which depends on p . But now we apply ι_5 and conclude that the same boundedness result holds for the backwards end of L_+ . Next, we apply Δ and conclude that the same boundedness result holds for the forwards end of L_+ . Putting these results together we see that L_+ is intrinsically bounded.

5.4 Local Convexity

Now we show that L_+ is locally concave near ∂L_+ except for 2 points on each boundary component. Given the properties of ι_5 and Δ , and symmetry, it suffices to prove that L'_+ is locally concave along the nice loop at all points of $\mathcal{U}_{ab} - \mathcal{U}_{cd}$. The corners are precisely $L_+ \cap (\mathcal{U}_{ab} \cap \mathcal{U}_{cd})$. Recall that $X_j = X_{F_j}$ is the Hamiltonian vector field associated to our invariant F_j . Let

$$Y = \alpha_1 X_1 + \alpha_2 X_2, \quad \alpha_1 = 1 + c - d, \quad \alpha_2 = 1 - c + d, \quad (44)$$

Let $\phi(a, b, c, d) = a + b - 1$ be the defining function for \mathcal{U}_{ab} . We already know that Y is tangent to L_+ . We compute that $Y \cdot \nabla \phi = 0$ when $\phi = 0$, which shows that Y is also tangent to \mathcal{U}_{ab} . Hence Y is tangent to the nice loop λ at points of \mathcal{U}_{ab} . The Hessian of the defining function is the matrix Q given by

$$Q_{ij} = \partial_{X_i} \partial_{X_j} \phi = X_i \cdot \nabla (X_j \cdot \nabla \phi). \quad (45)$$

Lemma 5.6 *The local convexity in the intrinsic metric is equivalent to the statement that*

$$q = Q(\alpha_1, \alpha_2) = \sum_{i=1}^2 \sum_{j=1}^2 Q_{ij} \alpha_i \alpha_j \neq 0 \quad (46)$$

at points along the nice loop.

Proof: Let $E : L_+ \rightarrow \mathbf{R}^2$ be the coordinate system giving the flat structure on L_+ . By construction $E_*(X_j) = e_j$, the j th coordinate vector field. The defining function for $E(\lambda)$ is given by $f = \phi \circ E^{-1} = 0$. The vector field $E_*(Y) = (\alpha_1, \alpha_2)$ is tangent to $E(\lambda)$. The curve f is locally convex $E(\lambda)$ at the point of interest if $Q(\alpha_1, \alpha_2) \neq 0$, where $Q_{ij} = \partial_i \partial_j f$ is the usual Hessian in the plane. But Q_{ij} agrees with the version given in Equation 45, by naturality. Thus, to test local convexity in the intrinsic metric, we just need to check that q in Equation 46 is nonzero. ♠

We compute that

$$q = \frac{8a(1-a)(1+c-d)^2(1-c+d)^2(c+d-1)(c+d-(c-d)^2)}{c^2d^2} < 0.$$

At points of $\mathcal{U}_{ab} - \mathcal{U}_{cd}$ we have $c + d - 1 < 0$ and all other terms are positive. Since $c, d \in (0, 1)$ we have $|c - d| < c + d$. So, the last factor in the numerator is positive. A single plot is enough to show that the negative sign determines concavity rather than convexity with respect to the side of the arc lying in L'_+ .

5.5 Extrinsic Nature of the Corners

We say that the *corners* of L_+ are the 4 points on the metric completion of L_+ , two on the front end and two on the back end, which are the meeting points of the concave arcs. We call these corners respectively the *forwards corners* and the *backwards corners*. In the next two results we compare the metric limit of a G -curve, with respect to the flat metric coming from the integrable structure, with the limit of the curve in \mathbf{R}^4 in the sense of Lemma 4.3. We call these two kinds of limits *intrinsic* and *extrinsic* respectively.

Lemma 5.7 *Let γ be a G -curve in L_+ . Then γ limits intrinsically on a back corner of L_+ if and only if the extrinsic backwards limit of γ is $(0, 0, 0, 0)$.*

Proof: Plugging in $b = 1 - a$ in the calculation of Lemma 5.4 we find that the numerators for b' and c' are $c + d - 1$. These are positive except at the corners of the nice loop λ , where they vanish. Likewise, the numerators for a' and d' are $a + b - 1$. In other words, ι_5 only maps the corners of the nice loop λ to $(0, 0, 0, 0)$. Let $\gamma' = \gamma \cap L'_+$. Then γ and γ' have the same backwards limits, both intrinsically and extrinsically. Also, γ' has the same forwards extrinsic and intrinsic limit on λ .

Suppose the backwards extrinsic limit of γ' is $(0, 0, 0, 0)$. From the calculation just mentioned, $\iota_5(\gamma')$ extrinsically and hence intrinsically limits on a corner of λ . Since ι_5 is an isometric involution of L'_+ , the curve γ' intrinsically limits on a backward corner of L'_+ (and L_+). If γ' intrinsically limits on a backwards corner of L_+ , then $\iota_5(\gamma')$ intrinsically and hence extrinsically limits on a corner of λ . The calculation in Lemma 5.4 now shows that $\gamma = \iota_5(\iota_5(\gamma))$ extrinsically limits on $(0, 0, 0, 0)$. ♠

Lemma 5.8 *Let γ be a G -curve in L_+ . Then γ limits intrinsically on a front corner of L_+ if and only if the extrinsic forwards limit of γ is $(1, 0, 1, 0)$.*

Proof: From our analysis of the previous lemma, there are exactly two G -curves of L_+ which hit the front corners of L_+ . We just have to check that the forwards limit of these are both $(1, 0, 1, 0)$. Suppose not. Then by Lemma 4.3, the forwards limit must be of the form $(1, 0, x, y)$ or $(x, y, 1, 0)$ for some $xy > 0$ and $x + y > 1$. We compute

$$\Delta(1, 0, x, y) = (0, b, b, 0), \quad \Delta(x, y, 1, 0) = (b, 0, 0, b), \quad b = \frac{2y}{2 + 2x}. \quad (47)$$

In this case $b \neq 0$ and we contradict the previous lemma. ♠

6 The Generic Convex Case

6.1 The Nature of the Convex Points

We carry out Steps 4 and 5 of the outline given in §2.8.

Recall that $L_+ \subset \mathcal{X}_+$ is one of our cylinder level sets. Let $C_+ = L \cap \mathcal{C}$. All points $(a, b, c, d) \in C_+$ satisfy $\min(a + b, c + d) > 1$. Hence C_+ is disjoint from the nice loop $\lambda \subset L_+$ and therefore lies to one side of it. The reader might want to glance at Figure 5 below before reading further.

Let \mathcal{V} denote the set of points (a, b, c, d) with $\min(a + b, c + d) = 1$. Let \mathcal{V}_{ab} denote the subset where $a + b = 1$ and likewise define \mathcal{V}_{cd} . The same proof as in Lemma 4.7 shows that $\nu_{ab} = \Sigma \cap \mathcal{V}_{ab}$ is a smooth 1-manifold away from the corners of the nice loop λ . The same goes for ν_{cd} . The symmetry I swaps ν_{ab} and ν_{cd} . So, one of them hits the (intrinsic) front end of L_+ if and only if the other one does. Let $\nu = \nu_{ab} \cup \nu_{cd}$. Let FL_+ denote the front end of L_+ , considered as a loop in the intrinsic metric completion of L_+ .

Lemma 6.1 *If ν does not hit the front end of L_+ then C_+ is an open cylinder bounded on one side by ν and on the other by FL_+ .*

Proof: The same argument as in Lemma 4.4 shows that each G -curve of L_+ can intersect ν_{ab} at most once. More strongly, a G -curve can only intersect $\nu = \nu_{ab} \cup \nu_{cd}$ once because going forwards it has already hit either λ_{ab} or λ_{cd} . For this reason, ν is a closed loop. Since each G -curve intersects ν at most once, each G -curve must intersect ν exactly once, and the region between ν and FL_+ is another cylinder. Every point in this cylinder satisfies $\min(a + b, c + d) > 1$ and no point outside this cylinder has this property. ♠

Lemma 6.2 *If ν does hit FL_+ then C_+ is a union of 2 topological disks, each bounded on 2 sides by arcs of ν and on two sides by arcs of FL_+ . One vertex of each component is a corner of λ and the opposite vertex is a corner of FL_+ .*

Proof: We rotate the picture so that the G -curves are vertical and the forwards direction is up. The points above ν near each corner belong to C_+ because they satisfy $\min(a + b, c + d) > 1$.

Consider an arc β of a G -curve that starts just above ν and runs backwards into ν . Since $\iota_3(C_+) = C(+)$ we see that $\iota_3(\beta)$ is a forwards moving G -curve in C_+ . We compute that $\iota_3(a, 1 - c, c, d) = (*, *, *, 0)$, a point not

in L_+ . Likewise $\iota_3(a, b, c, 1 - c) = (*, 0, *, *)$. But then $\iota_3(\beta)$ runs into FL_+ . Finally, $\iota_3(a, 1 - a, c, 1 - a) = (1, 0, 1, 0)$. We conclude from all this that C_+ contains a neighborhood of each corner of FL_+ . Moreover ι_3 maps the corners of λ to the corners of FL_+ .

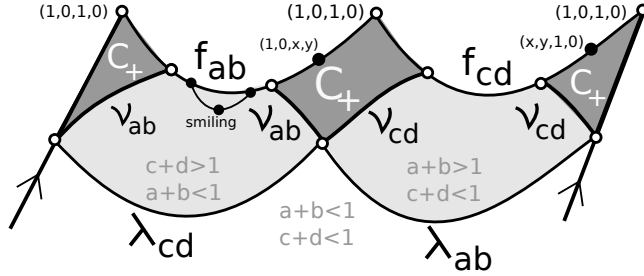


Figure 5: The relevant sets.

Now, FL_+ consists of two concave arcs α_{ab} and α_{cd} . Combining Lemma 4.3 and Lemma 5.8 we see that one of these arcs consists of points corresponding to the extrinsic limits of the form $(1, 0, x, y)$ with $xy > 0$ and $x + y > 0$. The other arc consists of points corresponding to extrinsic limits of the form $(x, y, 1, 0)$. One and the same arc cannot have both kinds of points because then by continuity it would contain $(1, 0, 1, 0)$, contradicting Lemma 5.8. We let α_{ab} be the arc containing points of the form $(1, 0, x, y)$. We let α_{cd} be the other arc.

Note that ν_{ab} cannot hit α_{cd} , because otherwise α_{cd} would contain points with extrinsic coordinates $(x, y, 1, 0)$ with $x + y = 1$, a contradiction. The fact that C_+ contains a neighborhood of the corners of FL_+ implies ν_{ab} cannot hit a corner of FL_+ .

No arc of ν_{ab} can join two points of α_{ab} . In this situation, the backwards convexity (“smiling”) of α_{ab} would force ν_{ab} to smile at some point. But the same calculation as in §5.4 shows that ν_{ab} is concave in the backwards direction – i.e. “frowning” everywhere. This is a contradiction.

Starting at the corners of λ , each arc of ν_{ab} cannot wind around L_+ in a nontrivial way, because no point of it can lie above λ_{ab} . The only thing that can happen is that each side of ν_{ab} goes more or less directly up and hits a point of α_{ab} . This gives exactly the topological picture shown in Figure 5.

In this situation, ν separates L_+ into two topological disks and a third region that contains λ . Each of these disks accumulates on a corner of λ_+ and a corner of the front end of L_+ . Finally C_+ cannot lie on both sides of μ . Hence C_+ is precisely the union of the two disk components. ♠

6.2 The Magic Formula

Here we establish Equation 24. Let $\tilde{L}_+ \subset \mathbf{R}^2$ be the universal cover of L_+ , given the intrinsic metric. The map I is an isometry of L_+ which preserves the ends, preserves λ , swaps the corners of L_+ and also swaps the corners of λ . From all this information, we conclude that I lifts to a translation of \mathbf{R}^2 which preserves \tilde{L}_+ and \tilde{C}_+ and $\tilde{\lambda}$ and moves the corners 1 click, so to speak. Figure 5, a hand-drawn cartoon, shows what we mean.

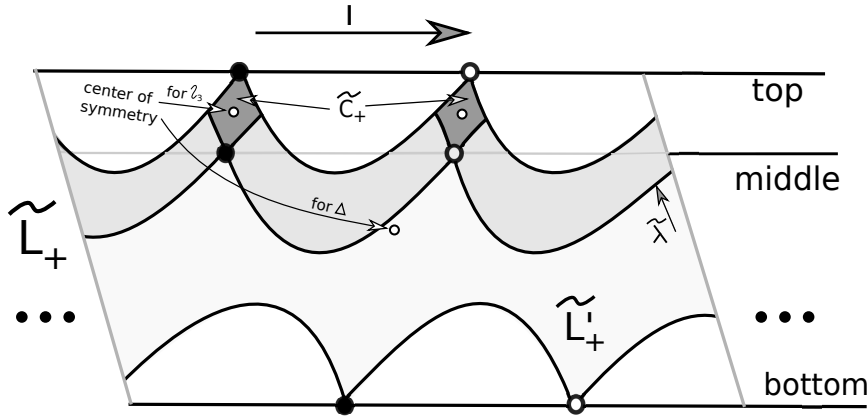


Figure 6: The lift to \mathbf{R}^2 .

Given the action of I , the lifts of the corners of either end of L_+ lie on straight lines. Likewise the lifts of the corners of λ lie on a straight line. We called these lines the top, bottom, and middle in our outline.

Lemma 6.3 *The middle line lies strictly between the top and bottom lines.*

Proof: We rotate so that our lines are horizontal and the top line is on top, as in Figure 5. Let L'_+ be the cylinder considered in the previous chapter. Because the ends of L'_+ are concave except at the corners, \tilde{L}'_+ lies between the middle and bottom lines, and only accumulates on these lines at the corners. Hence the middle line lies above the bottom line.

Suppose that the middle and top line coincide. Then the corners of $\tilde{\lambda}$ must lie on the top line. But the G -curves through the corners of λ continue for some time before exiting L_+ . In \mathbf{R}^2 the corresponding straight line segments travel upwards before exiting \tilde{L}_+ . Since \tilde{L}_+ lies below the top line, this means that the corners of $\tilde{\lambda}$ lie below the top line. ♠

Lemma 6.4 *Any lift of ι_3 to a map of \mathbf{R}^2 swaps the top and middle lines.*

Proof: Note that ι is defined on C_+ , a set which is either a cylinder or a union of 2 topological disks. In all cases, ι maps the corners of the nice loop to the corners of the front end and preserves C_+ .

In the cylinder case, ι_3 has 2 fixed points inside C_+ . The fixed points are centers of symmetry for C_+ . The lifts of these centers lie halfway between the top and middle lines. Hence any lift of ι_3 swaps the top and middle lines. In the disk case, we can replace ι_3 by $\iota' = \iota_3 \circ I$ if necessary to guarantee that the map fixes the two points which are the centers of symmetry of the two components of C_+ . We lift all these disks to \mathbf{R}^2 and we get an infinite row of isometric copies of these disks. Any lift we take will be a rotation about the center of one of the lifted disks. The center is halfway between the middle and top lines. So, we get the same result in the disk case for one of ι_3 or ι'_3 . But the result for one of the maps implies the result for the other. ♠

The action of ι_3 and Δ on \mathbf{R}^2 just described justifies Equation 24, the magic formula. This proves Theorem 1.1 for all convex generic 8-gons represented by points in \mathcal{X}_+ .

6.3 Getting to the Positive Part

Our proof of Theorem 1.1 is almost done in the generic convex case. We just have to justify our claim that we can always take a potential counter example to lie in \mathcal{X}_+ .

Recall from Lemma 2.2 that $\mathcal{C} - \mathcal{I} - \mathcal{I}^*$ has 4 components depending on the signs of $g_{ab} + g_{cd}$ and $g_{ab}^* + g_{cd}^*$. We denote these components by \mathcal{C}_{++} , etc. The first sign indicates the sign of $g_{ab} + g_{cd}$. The maps \sqrt{I} and J preserve each of $\mathcal{C}, \mathcal{I}, \mathcal{J}$. Thus each of these maps permutes our 4 components. Making a single evaluation is enough to verify the following action:

$$\begin{aligned} \sqrt{I} : & \quad \mathcal{C}_{++} \leftrightarrow \mathcal{C}_{--}, & \quad \mathcal{C}_{+-} \leftrightarrow \mathcal{C}_{-+}. \\ \sqrt{J} : & \quad \mathcal{C}_{++} \leftrightarrow \mathcal{C}_{+-}, & \quad \mathcal{C}_{-+} \leftrightarrow \mathcal{C}_{--}. \end{aligned}$$

Given any $p \in \mathcal{C} - \mathcal{I} - \mathcal{J}$ there is some word γ in I and \sqrt{J} such that $\gamma(p) \in \mathcal{C}_{++} \subset \mathcal{X}_+$. If p is a counterexample to Theorem 1.1, then so is $\gamma(p)$, because $\gamma(p)$ is affinely equivalent to p up to dihedrally relabeling.

This completes the proof of Theorem 1.1 in the generic case. The work in [21] takes care of the 8-gons with 4-fold rotational symmetry, and in the next chapter we will deal with the inscribed and circumscribed cases.

6.4 Behold the Torus

In this section we discuss without proof the full orbit of L_+ under the group $\langle A, \Delta \rangle$. Recall that $\iota_3 = A\Delta A$ and $\iota_5 = A\Delta A\Delta A$. We set

$$L_- = A(L_+), \quad M = \iota_3(L'_+). \quad (48)$$

These are both cylinders. We compute that

$$A(M) = A\iota_3(L'_+) = \Delta A(L'_+) = \iota_3(\iota_5(L'_+)) = \iota_3(L'_+) = M.$$

Thus Δ , ι_3 , and A are direction reversing isometries of L_+ , L_- , and M respectively. Figure 6 (which is partially plotted and partially hand-drawn) shows these cylinders in a presentation like Figures 3 and 4, for the invariants $(F_1, F_2) = (3, 4)$. In this case C_+ is a cylinder. The picture is a bit different when C_+ is a union of disks.

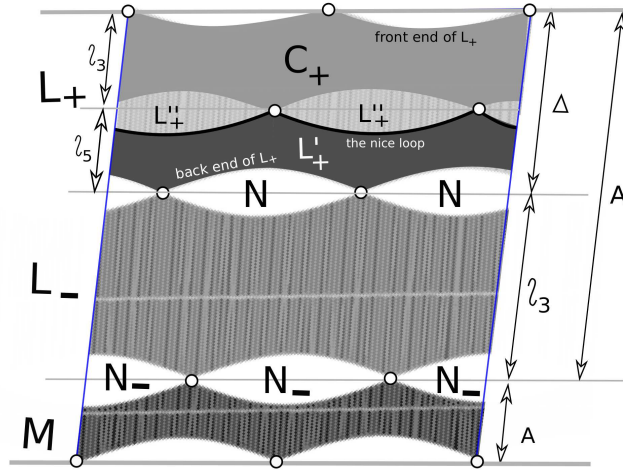


Figure 6: The various sets comprising \widehat{L} and the action on \widehat{L} .

Define

$$L''_+ = L_+ - C_+ - L'_+, \quad N = \iota_5(L''_+), \quad N_+ = \Delta(N), \quad N_- = \iota_3(N) \quad (49)$$

Then N and N_+ and N_- are respectively the regions between (L_+, L_-) and (L_+, M) and (L_-, M) . In Figure 6, which shows a case when C_+ is a cylinder, these interstitial regions are unions of two intrinsically convex disks, meeting at their two corners.

The union of all these pieces is a flat torus \widehat{L} , and the action of $\langle A, \Delta \rangle$, already defined on an open dense subset of \widehat{L} , extends to an isometric action of \widehat{L} . We can use this picture to get more information about the action of T_3 in terms of the invariant λ defined in §2.8.

Note that \widehat{L} has a canonical foliation by geodesics parallel to the ones containing the cusps. The maps A and Δ both preserve this foliation, and so T_3 does as well. There is some ambiguity in defining a fractional power of T_3 on \widehat{L} , but one can define any real power of T_3 on the leaf space \mathcal{L} of our foliation. Here \mathcal{L} is a circle whose length naturally is $2 + \lambda$ and T_3 acts as translation by λ . The quantity $\mu(p)$ names the point of \mathcal{L} containing p and the action of T_3 on \mathcal{L} is an extension of our magic formula. If we set

$$\beta = \frac{2 + \lambda}{\lambda}, \quad (50)$$

then T_3^β is the identity on \mathcal{L} .

We define the *conservative width* $w(C_+)$ to be the length of the subset of \mathcal{L} consisting of geodesics contained entirely in C_+ . When C_+ is a pair of disks, we have $w(C_+) = 0$. We could have $w(C_+) = 0$ even when C_+ is a cylinder, but when λ is small we probably have $w(C_+) \approx 1 - \lambda$. We define the *conservative subset* $C'_+ \subset C_+$ to be union of all the geodesic loops in our foliation which stay entirely inside C_+ . So C'_+ is a geodesic annulus bounded by geodesics in our foliation, and it has width $w(C_+)$.

Call a centrally symmetric convex octagon P *conservative* if it is represented by a point $p \in C'_+$. If P is conservative (and generically chosen, so that its full orbit is defined) then we will see $\text{floor}(w(C_+)/\lambda)$ consecutive convex octagons in its full orbit infinitely often. On the other hand, for any P represented by a point in L_+ , we will see at most $\text{floor}(1/\lambda)$ consecutive convex octagons in the full orbit. When λ is small, these upper and lower bounds will be close together.

What about the gaps between these runs of convexity? To get an integer we set $\beta' = \text{floor}(\beta)$. We have $T_3^{\beta'}(C'_+) \cap C'_+ \neq \emptyset$ provided that $w(C_+) > \lambda$. Indeed, if λ is small, these two sets will have large overlap. What this means is that, in these cases, we can find plenty of centrally symmetric octagons represented by points in C'_+ such that the (β') th power of T_3 makes them convex again. So, consecutive runs of these convex octagons in the full orbit are have indices shifted by about β' . This is the kind of strong periodicity you get from translation on a flat torus.

I want to emphasize that everything in this section is speculative and tentative. I just thought it would be nice to explain some of the picture beyond the statement of the Main Theorem.

7 The Inscribed and Circumscribed Cases

We carry out Step 6 of our outline in §2.8 and thereby finish the proof of Theorem 1.2. We also prove Theorem 1.3. Let \mathcal{CI} and \mathcal{CI}^* respectively be the set of inscribed and circumscribed convex points.

Lemma 7.1 *\mathcal{CI}^* is forward T_3 -invariant.*

Proof: The defining equation for \mathcal{I}^* is $a - b + c - d = 0$. A calculation shows that this is T_3 invariant. Hence \mathcal{I}^* is T_3 -invariant. (Again, this is a special case of a result in [2].) We just have to show that $T_3(\mathcal{CI}^*) \subset \mathcal{C}$.

Our argument works for any convex circumscribed n -gon P_0, \dots, P_{n-1} with $n \geq 7$. When P is the regular n -gon, $T_3(P)$ is convex. If we had some counter-example, then by continuity, we could find an example where the lines $\overline{P_j P_{j+3}}$, for $j = 0, 1, 2$, have a triple intersection. But then, by the converse to Brianchon's Theorem, the hexagon P_0, \dots, P_5 is also inscribed in the same ellipse E as is P . In particular, $\overline{P_0 P_5}$ is tangent to E . Since only 2 lines containing P_0 are tangent to E , either P_0, P_1, P_5 are collinear or $P_{n-1} P_0 P_5$ are collinear. Either statement violates the convexity of P . ♠

The space \mathcal{I}^* is partitioned into the planes Π_k consisting of points of the form $(x + k, x - k, y - k, y + k)$. Let

$$h = -g_{ab} \circ (A\Delta)|_{\Pi_k} = \frac{4k^3 - x + y - 4kxy}{(k - x)(k + y)}. \quad (51)$$

Let $L(k, \ell) \subset \Pi_k$ be the level set $h^{-1}(\ell)$.

Lemma 7.2 *$L(k, \ell) \cap \mathcal{CI}^*$ is non-empty only if $(k, \ell) \in \mathcal{K}$.*

Proof: Let $(a, b, c, d) = (x + k, x - k, y - k, y + k)$. The convexity requirement that $|a - b| < 1$ gives $|k| < 1/2$. Suppose that (a, b, c, d) represents a convex point. Then so does $A\Delta A(a, b, c, d)$. We compute

$$g_{ab} \circ A\Delta|_{\mathcal{I}^*} = g_{ab} \circ A\Delta A \circ IJ|_{\mathcal{I}^*},$$

where I and J are the maps from Equation 5. But $A\Delta A$ preserves convexity by Lemma 2.3. If $(a, b, c, d) \in \mathcal{C}$ then $IJ(a, b, c, d) \in \mathcal{C}$ and hence $(a', b', c', d') \in \mathcal{C}$. But then $a' + b' > 1$ and this gives $g_{ab}(a', b') < 2$. ♠

Lemma 7.3 T_3^4 preserves $L(k, \ell)$ and the action, when complexified, is conjugate to a linear fractional transformation acting on the Riemann sphere.

Proof: A direct (but large) calculation shows that $T_3^2(\Pi_k) = \Pi_{-k}$ and $h(T_3^2(p)) = -h(p)$ for $p \in \mathcal{I}^*$. Hence T_3^4 preserves $L(k, \ell)$. Solving the equation $h(x, y) = \ell$ and clearing denominators, we get the quadratic equation

$$(\ell - 4k)xy + (1 + k\ell)x - (1 + k\ell)y - (4k^3 - k^2\ell). \quad (52)$$

This defines a projective curve in \mathbf{CP}^2 biholomorphic to the Riemann sphere. Under this identification, the holomorphic automorphism T_3^4 is a linear fractional transformation. ♠

Let $\phi_{k,\ell}$ be the linear fractional transformation conjugate to the action extending T_3^4 on $L(k, \ell)$. Let \mathcal{K} denote the set of parameters (k, ℓ) with $|k| < 1/2$ and $|\ell| < 2$.

Lemma 7.4 If $(k, \ell) \in \mathcal{K}$ then $\phi_{k,\ell}$ is a hyperbolic linear transformation. The attracting fixed point is convex Poncelet and the repelling fixed point is (up to rotation) the star-reordering of the attracting fixed point.

Proof: In $L(k, \ell)$ we can directly solve the equation $\phi_{k,\ell}(z) = z$ for x and y . There are (formally) two solutions $(x_0, -y_0)$ and $(y_0, -x_0)$, where

$$x_0 + y_0 = \frac{2(4k - \ell)(k\ell - 1)}{(2 + \ell)(2 - \ell)}, \quad x_0 y_0 = \frac{-2 - 4k + 4k\ell - k^2\ell^2}{(2 + \ell)(2 - \ell)}. \quad (53)$$

The polynomial $t^2 - (x_0 + y_0)t + x_0 y_0$ has discriminant

$$D = 4(1 + 4k^2 - 2k\ell)((8 - \ell^2) - 8k\ell + 4(k\ell)^2). \quad (54)$$

We have $D > 0$ when $(k, \ell) \in \mathcal{K}$. Thus we get 2 distinct real solutions. A calculation shows that $g_{ab} + g_{cd} = 0$ for the solutions. Since $g_{ab}^* + g_{cd}^* = 0$ as well, any non-degenerate fixed point is Poncelet.

The map $\phi_{k,\ell}$ has 2 real fixed points and is real linear. Hence $\phi_{k,\ell}$ is either hyperbolic or elliptic of order 2. Since \mathcal{K} is connected and $\phi_{k,\ell}$ varies continuously and the elliptic case is isolated, the elliptic option either always occurs or never occurs. Since it does not always occur, it never occurs.

The fixed points have the form (a, b, c, d) and $-(c, d, a, b)$. Up to rotation, the corresponding polygons are star-reorderings of each other. Given the

forward invariance of \mathcal{CI}^* , one of the fixed points (a, b, c, d) is the limit of convex 8-gons in $L(k, \ell)$. This gives us

$$|a - b| = |k| < 1, \quad |c - d| = k < 1, \quad a + b \geq 1, \quad c + d \geq 1.$$

If $a + b = 1$ then $g_{ab}(a, b, c, d) = 2$. But then $g_{cd}(a, b, c, d) = -2$. This is not possible for a finite pair (c, d) . Hence $a + b > 1$. Likewise $c + d > 1$. Hence (a, b, c, d) gives a nontrivial convex 8-gon. From the calculation above, this 8-gon is Poncelet. The other fixed point is thus star-convex Poncelet. Given the forward invariance of \mathcal{CI}^* , the convex fixed point must be attracting. ♠

Thus, the backwards T_3^{4n} iterates of any point of $\mathcal{CI}^* - \mathcal{CI}$ either accumulate on a star-convex 8-gon or become undefined. In either case, the backwards T_3 -orbit of any point of $\mathcal{CI}^* - \mathcal{CI}$ eventually exits \mathcal{CI}^* . Dually, the forwards T_3 -orbit of any point of $\mathcal{CI} - \mathcal{CI}^*$ eventually exits \mathcal{CI} . This completes Step 6 of the outline in §2.8. Our proof of Theorem 1.2 is done.

Since T_3 is the identity on Poncelet polygons up to relabeling, we see that T_3 has the same convergence properties as T_3^4 . This finishes the proof of Theorem 1.3.

References

- [1] A. I. Bobenko, T. Hoffmann, Yu. B. Suris, *Hexagonal circle patterns and integrable systems: patterns with the multi-ratio property and Lax equations on the regular triangular lattice*, arXiv:0104244 (2001)
- [2] L. S. Evans and J. F. Rigby *Octagrammum Mysticum and the Golden Cross Ratio*, The Mathematical Gazette, Vol 86, No 505 (Mar. 2002) pp 35-43
- [3] M. Glick, *The Limit Point of the Pentagonam Map*, International Mathematics Research Notices 9 (2020) pp. 2818–2831
- [4] M. Glick, *The pentagram map and Y-patterns*, Adv. Math. **227**, 2012, pp. 1019–1045.
- [5] M. Gekhtman, M. Shapiro, S. Tabachnikov, A. Vainshtein, *Higher pentagram maps, weighted directed networks, and cluster dynamics*, Electron. Res. Announc. Math. Sci. **19** (2012), pp. 1–17
- [6] L. Halbeisen and N. Hungerbühler, *A Simple proof of Poncelet’s Theorem (on the occasion of its bicentennial)* Amer. Math. Monthly, **122** No. 6, (2015) pp 537-551
- [7] A. Izosimov, *The pentagram map, Poncelet polygons, and commuting difference operators*, arXiv 1906.10749 (2019)
- [8] B. Khesin, F. Soloviev *Integrability of higher pentagram maps*, Mathem. Annalen. Vol. 357 no. 3 (2013) pp. 1005–1047
- [9] B. Khesin, F. Soloviev *The geometry of dented pentagram maps*, J. European Math. Soc. Vol 18 (2016) pp. 147 – 179
- [10] Wolfram Research Inc., *Mathematica*, Wolfram Programming Lab, Champaign, IL (2021)
- [11] G. Mari Beffa, *On Generalizations of the Pentagonam Map: Discretizations of AGD Flows*, Journal of Nonlinear Science, Vol 23, Issue 2 (2013) pp. 304–334
- [12] G. Mari Beffa, *On integrable generalizations of the pentagram map* Int. Math. Res. Notices (2015) (12) pp. 3669-3693
- [13] Th. Motzkin, *The pentagon in the projective plane, with a comment on Napier’s rule*, Bull. Amer. Math. Soc. **52**, 1945, pp. 985–989.

- [14] V. Ovsienko, R. E. Schwartz, S. Tabachnikov, *The pentagram map: A discrete integrable system*, Comm. Math. Phys. **299**, 2010, pp. 409–446.
- [15] V. Ovsienko, R. E. Schwartz, S. Tabachnikov, *Liouville-Arnold integrability of the pentagram map on closed polygons*, Duke Math. J. Vol 162 No. 12 (2012) pp. 2149–2196
- [16] B. Rodin and D. Sullivan, *The Convergence of Circle packings to the Riemann Mapping Theorem*, J. Diff. Geom. **26** (1987) pp. 349–360
- [17] O. Schramm, *Rigidity of Infinite (circle) Packings*, J.A.M.S., Vol 4, No. 1, (1991) pp 127–149
- [18] R.E. Schwartz, *The pentagram map*, Exper. Math. **1**, 1992, pp. 71–81.
- [19] R. E. Schwartz, *Discrete monodromy, pentagrams, and the method of condensation*, J. of Fixed Point Theory and Appl. **3**, 2008, pp. 379–409.
- [20] R. E. Schwartz, *The Poncelet Grid*, Advances in Geometry Vol. 7 (2006) pp. 157-175
- [21] R. E. Schwartz, *Survey Lecture on Billiards*, Proceedings of the 2002 International Congress of Mathematicians, I.M.U. Press (2021)
- [22] R. E. Schwartz, *A Textbook Case of Pentagram Rigidity*, arXiv 2108-07604 preprint (2021)[
- [23] R. Schwartz, S. Tabachnikov, *Elementary surprises in projective geometry*, Math. Intelligencer Vol. 32 (2010) pp 31–34.
- [24] J. Silverman, *The arithmetic of dynamical systems*, Graduate Texts in Mathematics **241** (2007) Springer
- [25] F. Soloviev *Integrability of the Pentagram Map*, Duke Math J. Vol 162. No. 15, (2012) pp. 2815 – 2853
- [26] M. Weinreich, *The Algebraic Dynamics of the Pentagram Map*, (2021) arXiv: 2104.06211